2017

Evaluation of floodwater loading on domestic housing

Kail, S.

Kail, S. (2017) 'Evaluation of floodwater loading on domestic housing', The Plymouth Student Scientist, 10(2), p. 80-133.
http://hdl.handle.net/10026.1/14162

The Plymouth Student Scientist
University of Plymouth

Evaluation of floodwater loading on domestic housing

Samuel Kail

Project Advisor: David Easterbrook, School of Marine Science and Engineering, Plymouth University, Drake Circus, Plymouth PL4 8AA

Abstract

Floodwater pressure on domestic housing can cause damage or collapse. With the increased use of property level protection, more property owners are taking actions to limit water ingress at the cost of increased floodwater pressure differential on property walls. Currently CIRIA and the Environment Agency advise that properties should be protected up to a maximum of 0.6m (CIRIA, 2007). This protection height is currently used in industry as the standard protection height in property level protection schemes. The general consensus from sources referenced in a literature review was that most domestic properties are capable of supporting 0.6 meters of flood water, but any higher than this and inspection should be carried out by a qualified building surveyor, architect or structural engineer (ODPM, 2003). This study analysed a number of characteristics for a masonry wall panel, 4 meters wide and 2.5 meters high, incorporating an inner and outer leaf both 100mm thick. The analytical methods utilised were yield line analysis, finite element modelling and the design moment of resistance equation, which were conducted with the aim of arbitrating whether the current industry standard protection height of 0.6m is appropriate. The panel analysed was deemed suited to resisting loading from a static 0.6m head of water, providing the panel is in a condition which would not compromise the design flexural strength or material factor; and there are no large openings protected with property level protection barriers, which demonstrated an increase in maximum bending moment. In the presence of hydrodynamic loading, the wall panel was deemed suited to a protection height of 0.6m providing the velocity component orthogonal to the panel is less than 0.03m/s. The panel was deemed suitable within these limits because the panel section modulus, width, support conditions and vertical loading are all within the relevant ULS identified. However, areas have been identified for further study, including study of further yield line patterns outside of the scope of this study, in order to increase the confidence in this arbitration. It was found that the current industry standard protection height of 0.6m would not be appropriate for all properties however, due to the huge variety in masonry panel characteristics. The results from this study can be used in the design of future domestic properties at risk of flooding, as well as in the protection of existing properties at risk of flooding.

Contents

Appendix G - Original panel modelled as beam with fixed supports spanning vertically

Appendix H - Tabulated yield line analysis results for maximum bending moment with varying panel width

Appendix I1 - 1m wide wall panel yield line calculation

Appendix I2 - 2m wide wall panel yield line calculation

Appendix I3 - 6m wide wall panel yield line calculation

Appendix I4 - 8m wide wall panel yield line calculation

Appendix I5 - 10m wide wall panel yield line calculation

Appendix J - Free top edge yield line analysis calculation

Appendix K1 - Opening for door frame yield line calculation

Appendix K2 - Opening for window frame yield line calculation

Appendix K3 - Opening for large sliding door frame yield line calculation

Appendix L - Characteristic compressive strength of masonry calculation

Appendix M - Moment of resistance parallel to the bed joints calculations for different applied vertical loads

Appendix N - Tabulated design moment of resistance results for varied vertical loading (applied as a floor loading to $12m^{2)}$

Appendix O1 - Resultant stress contour of the original panel under applied vertical loading from $12m^2$ with a loading of $0kN/m^2$

Appendix O2 - Resultant stress contour of the original panel under applied vertical loading from $12m^2$ with a loading of $1kN/m^2$

Appendix O3 - Resultant stress contour of the original panel under applied vertical loading from $12m^2$ with a loading of $2kN/m^2$

Appendix O4 - Resultant stress contour of the original panel under applied vertical loading from $12m^2$ with a loading of $3kN/m^2$

Appendix O5 - Resultant stress contour of the original panel under applied vertical loading from $12m^2$ with a loading of $4kN/m^2$

Appendix O6 - Resultant stress contour of the original panel under applied vertical loading from $12m^2$ with a loading of $5kN/m^2$

Appendix P - Flood water hazard matrix

Appendix Q - Hydrodynamic loading results

Appendix R - Maximum bending moment for varying velocities orthagonal to the wall panel calculations

Appendix S - Velocity component orthagonal to the wall panel verses maximum bending moment for slower velocities observed

Appendix T - Check sheet to assist in determining whether a protection height of 0.6 meters is appropriate for a wall panel

i. List of Tables

ii. List of Figures

iii. List of Graphs

iv. List of Notation and Abbreviations

A	Area (m^2)
C_D	Coefficient of drag
$CIRIA$	Construction Industry Research and Information Association
EA	Environment Agency
EWD	External work done
f_b	Normalised mean compressive strength of brick units (N/mm^2)
f_K	Characteristic compressive strength of masonry (N/mm^2)
f_m	Mortar strength (N/mm^2)
f_{xk1}	Characteristic flexural strength of masonry bending about an axis parallel to the bed joints (N/mm^2)
F	Force (kN)

FEA	Finite Element Analysis
g	Gravitational acceleration (9.81m/s^2)
h	Head, depth of water surface (m)
h_G	Depth to centroid of wetted area (m)
IWD	Internal work done
M_p	Plastic moment of resistance per unit length (kNm/m)
$M_{Rd,1}$	Design moment of resistance parallel to the bed joints (kNm/m)
PLP	Property Level Protection
SLS	Serviceability Limit State
u	Intensity of the velocity component orthoganol to surface (m/s)
ULS	Ultimate Limit State
Z	Section modulus (mm^3)
γ_M	Appropriate partial factor for materials
ρ	Mass density (1000kg/m^3 assumed for water)
σ_d	Design vertical load per unit area (N/mm^2)

1. Introduction (Aims and Objectives)

A growing number of households are adopting water exclusion strategies with the aim of preventing the ingress of flood water during flood events, using property level protection (PLP) products such as door barriers and non-return valves (CIRIA, 2007). This strategy comes at the expense of an increased pressure differential on the property walls, as flood water can no longer be equalised inside the property. This risk of damage and collapse increases with increased protection height before flood water is allowed to enter the property. In order to provide greatest protection to a property during a flood event using PLP measures, it is necessary to find a limit of protection (limit of loading) before damage to the walls and other structural features occurs, so that floodwater ingress can be restricted up to this level and allowed to enter from this point onwards. This may be described as a hybrid between a water exclusion and a water entry strategy, minimising water entry whilst maintaining structural integrity (CIRIA, 2007).

Figure 1: Brickwork wall broken from behind by flood water in Malton, U.K. (Kelman, 2000)

A literature review revealed that according to the majority of the sources referenced, most walls in domestic properties are capable of supporting 0.6 meters head of water, but any higher than this and inspection should be carried out by a qualified building surveyor, architect or structural engineer (ODPM, 2003). This figure is also used in current EA (Environment Agency) and CIRIA guidance and has been used as the standard protection height in recent property level protection (PLP) schemes (CIRIA, 2007). It was therefore decided that this flood protection height would form the base of analysis, since it had the most recommendations from various respected bodies and organisations and is currently being used as the industry standard.

Yield line analysis (plastic analysis) and elastic analysis methods of calculating maximum bending moment were explored, revealing that for the purposes of this work, yield line analysis should be used in hand calculations since the use of elastic analysis for panels with irregular shapes or loading, or which contain large openings is very arduous (Meyboom, 2002; Reynolds *et al.*, 2008). However, finite element analysis (FEA) software allows elastic analysis techniques to be used on these more complicated panels quickly and easily, and were used in this study through the use of LUSAS (Reynolds *et al.*, 2008). In using two methods of calculating maximum bending moments it was hoped that successful correlation of results and therefore validation would increase the reliability.

Research was undertaken into the design moment parallel to the bed joints equation, including consideration of panel depth and the effect of wall ties. Due to the range of varying factors between different property walls, it was deemed difficult to justify applying design moment calculations to the majority or a defined segment of properties unless a conservative approach was adopted.

Finally, the impacts of using property level protection (PLP) products in wall panel openings was explored, and other factors which are important in the ability of a wall to resist hydrostatic and hydrodynamic forces were considered for future investigation.

A literature review and a previous project outlined several objectives for subsequent study, as follows: to continue on the preliminary analysis carried out on the wall panel observed previously with the aim of obtaining a broader range of results; to produce a finite element model of this same panel for comparison and validation using LUSAS; and to further this research through the analysis of the following common housing features and other variables, using either yield line analysis and finite element modelling or the moment resistance equation where applicable:

- Altered widths
- Altered support conditions
- Addition of openings and PLP measures
- Vertical loading
- Masonry construction
- Masonry age and condition
- Hydrodynamic loading

These objectives will be fulfilled with the aim of developing increased understanding of how flood water impacts domestic property walls, by analysing the impact on the maximum applied bending moment and the design moment of resistance. The results gained from this study will then be assessed to fulfil the ultimate aim of arbitrating whether the current industry standard protection height of 0.6 meters is appropriate for domestic properties. These findings can then be used in the design of future domestic properties at risk of flooding, as well as in the protection of existing properties at risk of flooding.

Whilst other works, many referenced in this paper, have investigated the head of water domestic properties are capable of supporting, this study is unique in that it examines a single protection height across a range of variables, challenging the current industry guidance.

2. Research and Analysis

2.1. Continuing Preliminary Analysis Conducted in previous research

The sizing of the masonry wall panel examined was 4m wide and 2.5m high, incorporating an inner and outer leaf both 100mm thick, consisting of clay masonry units with over 12% water absorption, and using M4 mortar (see Appendix A for

elevation and section). It was also assumed that both leaves of the wall would act together i.e. there would be effective wall ties, all of which were considered to be reasonably representative for domestic properties. The design moment parallel to the bed joints was calculated as 0.333kNm/m in a pre-study project (calculations shown in Appendix B).

Analysis into the maximum bending moment in the panel detailed was completed using both yield line analysis and FEA.

2.1.1. Continued Yield Line Analysis Calculations

It was previously suspected that the maximum bending moment in the panel will be observed when the centre horizontal yield line is roughly central, as illustrated in Figure 2, and the maximum bending moment would reduce when this horizontal yield line is either lowered or raised. This prediction was derived from a number of sources, including Kelman and Spence (2003), who reported the use of a similar yield line pattern in their analysis, and others who suggested that this was a likely yield line pattern for masonry with continuous supports under lateral loading; including Brincker (1984) and Morton (1985). This was coupled with personal intuition that failure will be more likely towards the centre due to increased distance from the supports.

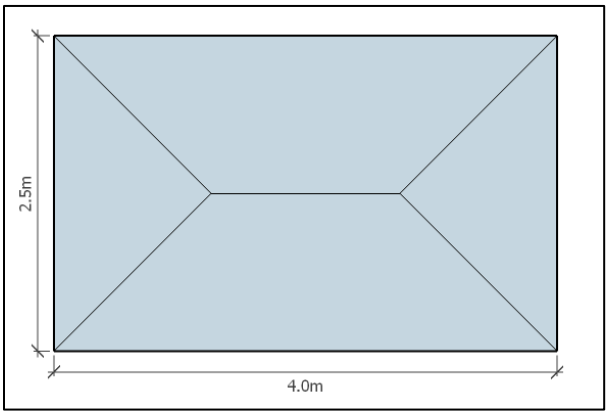

Figure 2: Common yield line pattern for panels with continuous supports under lateral loading

Analysis was previously carried out on four different yield line patterns, with lower diagonal yield lines at 45 degrees to the horizontal of height/width 0.5m, 0.6m, 0.7m and 0.8m. The lower diagonal yield lines were angled at 45 degrees at the base of the wall because it was found that this is a common yield line angle, where permitted by the panel shape, which provides a fairly accurate distribution of loads (Goodchild and Kennedy, 2003). It was thought that the lower diagonal yield lines should be angled at 45 degrees rather than the upper diagonal yield lines, since the lower yield lines were under direct loading. Diagonal yield lines were angled at 45 degrees at the base of the panel throughout all of the analysis in order to produce results which would be more easily comparable and to help maintain a focus to the research. Thus, several additional patterns were investigated as part of this study with the height/width of the lower diagonal yield lines ranging up to 2m, at which point these yield lines met in the middle, as illustrated below in Figure 3. The results for the maximum bending moment for all of these yield line patterns is displayed in Graph 1 below, and in a tabular format in Appendix C. The full yield line analysis calculations for each of the yield line patterns used are located in Appendix D.

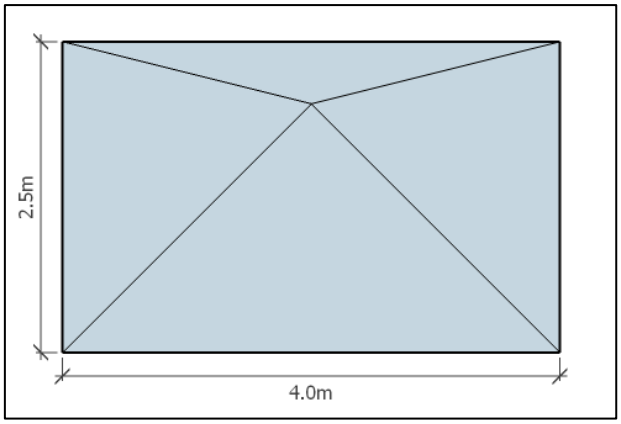

Figure 3: Yield line pattern with lower diagonal yield lines of height/width 2.0m

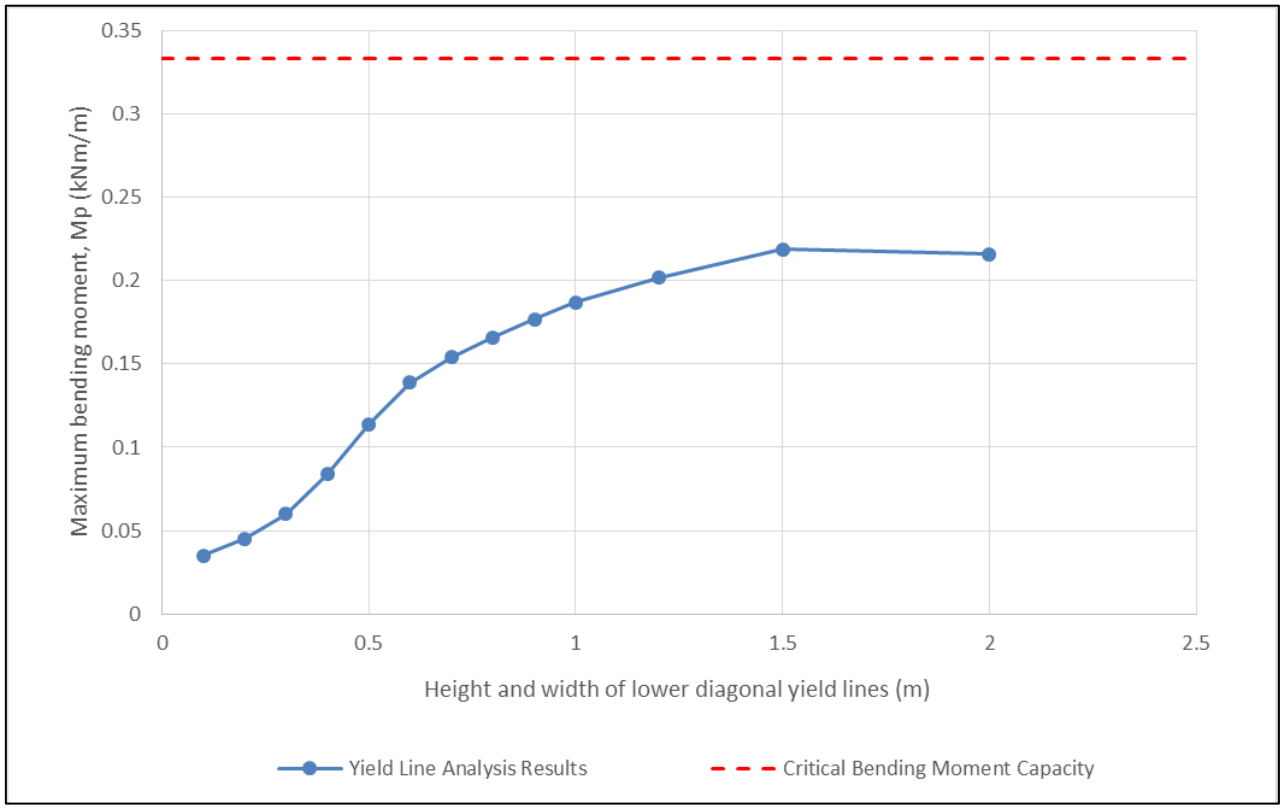

Graph 1: Maximum bending moments for varying yield line patterns

In contrast to previous predictions, the maximum bending moment continues to increase as the lower diagonal yield lines (at 45 degrees to the horizontal) increase in length up to 1.5m. Increases in length from this point cause a slight reduction in maximum bending moment up to the point where the two lower diagonal yield lines meet (i.e. 2.0m high/wide). When the lower diagonal yield lines are 1.5m in length, as shown in Figure 4, this produced the highest maximum bending moment of all of the yield line patterns analysed, calculated as 0.219kNm/m. Whilst at this stage it is unknown whether this is the yield solution, this is lower than the resistance moment for the wall, 0.333kNm/m, calculated in a pre-study project (calculations shown in

Appendix B), suggesting that the wall would not fail with hydrostatic loading from 0.6 head of water, with a factor of safety of 1.5.

Graph 1 illustrates that the increase in maximum bending moment with increased length of the lower diagonal yield lines up to 1.5m is non-linear. From lower diagonal yield line lengths of 0.1m to 0.5m, the increases in the maximum bending moment appears almost exponential. From 0.5m to 1.5m the maximum bending moment increases but less and less. From a lower diagonal yield line length of 1.5m the maximum bending moment very marginally begins to reduce. Lower diagonal yield lines below the minimum length of 0.1m examined in the study were not thought to produce higher bending moments judging from the correlation of the results shown in Graph 1. Furthermore, these shorter yield lines were thought to be unlikely failure patterns due to the very close proximity of horizontal cracking these patterns would require, with a spacing verging on the height of a single brick layer and large angle to the horizontal of the upper diagonal yield lines which may not produce accurate distribution of loads (Goodchild and Kennedy, 2003).

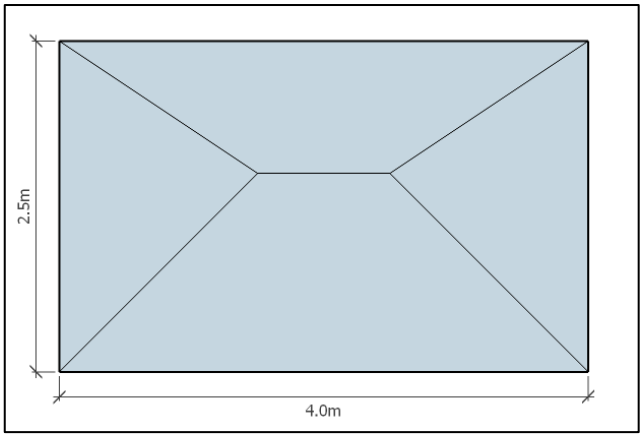

Figure 4: Yield line pattern which produced the highest bending moment

The yield line pattern which produced the highest bending moment, as shown in Figure 4 above does not seem to closely correlate with previous yield line patterns proposed in research carried out by Kelman and Spence (2003), or yield line patterns proposed by others such as Morton (1985) and Brincker (1984). It is however a viable yield line pattern because the bending moment value it provides (0.219kNm/m) is less than that calculated using approximate analysis of the panel modelled as a simply supported beam spanning vertically (0.947kNm/m), using the Steel Designers' Manual (Davison and Owens, 2012) (as depicted in a schematic and calculated in Appendix E).

Whilst it was predicted that the yield line depicted in Figure 2 would produce the highest maximum bending moment, it was expected that the value of maximum bending moment would be visible as a peak in Graph 1 as it has. The supposition arising from these results not documented elsewhere is that the maximum bending moment increases with increased length of the lower diagonal yield lines up to the maximum point with lower diagonal yield lines at 1.5m as depicted in Figure 4, for the wall panel observed.

The trend of increased maximum bending moment with increased length of lower diagonal yield lines up until the maximum bending moment value is due to a reduction

in the internal work done relative to the external work done in the yield line analysis calculations. Yield line analysis fails to consider the distribution of loading on the wall panel however. This demonstrates that, whilst the yield line solution should be that which provides the critical moment (the highest moment or the least load capacity), there is a requirement to consider the appropriateness and likelihood of the solution given the "conditions encountered and the problem defined" (Goodchild and Kennedy, 2003; Kelman and Spence, 2003:60). This complicates the use of yield line analysis, since whilst there are a number of suggested yield line patterns, the appropriateness of a particular yield line pattern for a particular scenario (i.e. certain boundary conditions and loading) is somewhat down to engineering judgement, and thus the analysis becomes less of an exact science and more of an art. This observation highlights that the reliable use of yield line analysis requires experience and "sound understanding of theory" in order to identify a likely failure mechanism (Caprani, 2006; Cobb, 2014:70). Previously it was thought that a simple trial-and-error approach would be appropriate to find the critical moment, however this is unsuitable given the results.

Perhaps the closest yield line pattern to that which yielded the highest maximum bending moment in this analysis (as shown in Figure 4) which has been previously proposed is that shown below in Figure 5, proposed by Kelman and Spence (2003), Bhatt *et al.* (2014) and Reynolds *et al.* (2008), since the lower diagonal yield lines are relatively long and come close to the centre of the panel. Whilst this provides a potential solution, Bhatt *et al.* (2014) and Reynolds *et al.* (2008) suggest the use of this yield line pattern for the case where one edge is free and the others are fixed (hence this pattern is used in Section 2.3.2 under these support conditions).

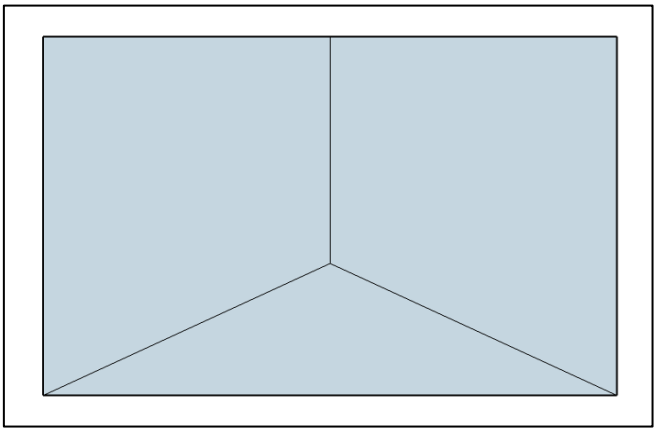

Figure 5: Yield line pattern suggested by Kelman and Spence (2003)

On consideration of the most appropriate yield line solution for the wall panel under examination, personal engineering judgement favours a yield line pattern comparable to that illustrated in Figure 6 below, or a similar variation where there is a concentration of yield line around the applied loading. This is because personal judgment would suggest this area is probably the most likely to crack; an opinion seemingly carried by Kelman and Spence (2003), who used a similar yield line pattern in their analysis. The results show that a yield line pattern similar to that shown in Figure 6 (perhaps with 0.7m high/wide lower diagonal yield lines) does not produce the highest bending

moment of the patterns analysed, highlighting the need for validation, through the use of finite element analysis (see Section 2.1.2).

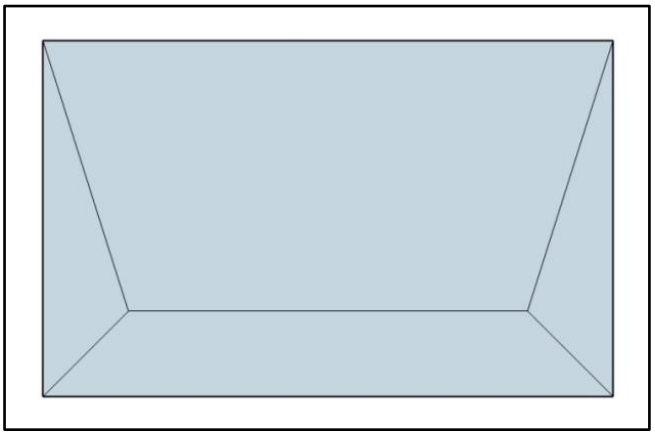

Figure 6: Perhaps more likely representation of the yield line pattern with continuous supports under relatively shallow hydrostatic loading

2.1.2. LUSAS Model (FEA)

The LUSAS model created replicated the wall considered in the yield line analysis. The wall was modelled as a thick shell, with fully fixed support conditions on all sides as in the yield line analysis. Masonry was not a material option in the academic version of LUSAS, so concrete was deemed to be the closest match available. It is important to consider that the Young's modulus of the concrete used in LUSAS is $30*10^6$ kN/m^2, whereas the Young's modulus of masonry will vary since the material is non-homogeneous. Whilst there will be some difference in the maximum bending moment in the model due to differing elastic deformation, a parametric study using different Young's Modulus values revealed that this difference would be negligible. The self-weight of the material was applied for greater realism of the testing. Figure 7 illustrates the model mesh with labelled nodes. An element size of 0.1m^2 was used for the mesh, resulting in a total of 1066 nodes for the panel observed. Initially a less refined mesh size was used (i.e. less divisions and nodes) however this provided results fairly distant from those obtained with a more highly refined mesh, hence the higher refinement of 0.1m^2 was adopted. Higher mesh refinements result in longer model runs which could have been an issue in the past with less powerful computers available, however this is less of an issue today, with the size of the model resulting in negligible difference in run times between the lower and higher refined models. It was noted that further increasing the refinement of the model could increase the accuracy of the results, however this was found to make little difference to the results.

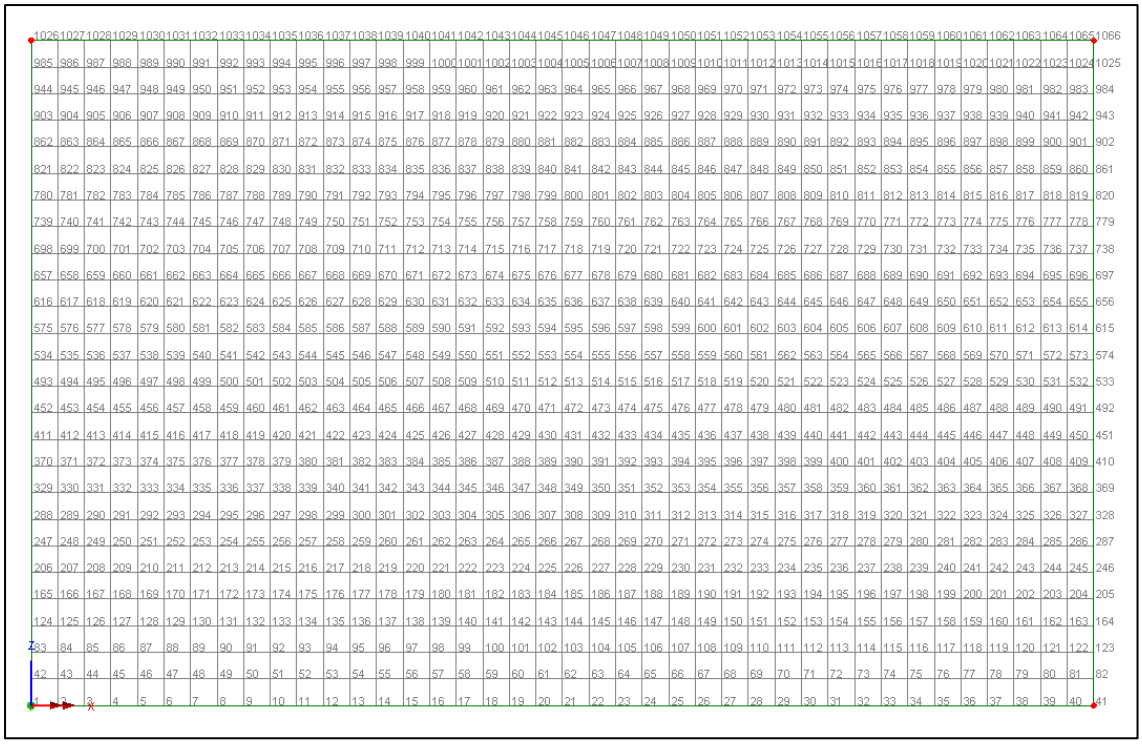

Figure 7: Model mesh with labelled nodes

In order to apply hydrostatic pressure to the model, a discrete four node patch load was applied, essentially creating a triangular load along the base of the panel, as illustrated in Figure 8. This required the pressure (kN/m^2) at the surface of the flood water adjacent to the wall (0.6m high) and the pressure at the bottom of the wall, and LUSAS would linearly interpolate between these values. The pressure applied at the surface of the flood water is zero kN/m^2, however the pressure at the bottom of the wall is calculated using Equation 1, where h corresponds to the depth of the water (Hamill, 2011):

$$(\mathbf{1})\ Pressure = \rho * g * h = 1000 * 9.81 * 0.6 = 5.886 kN/m^2$$

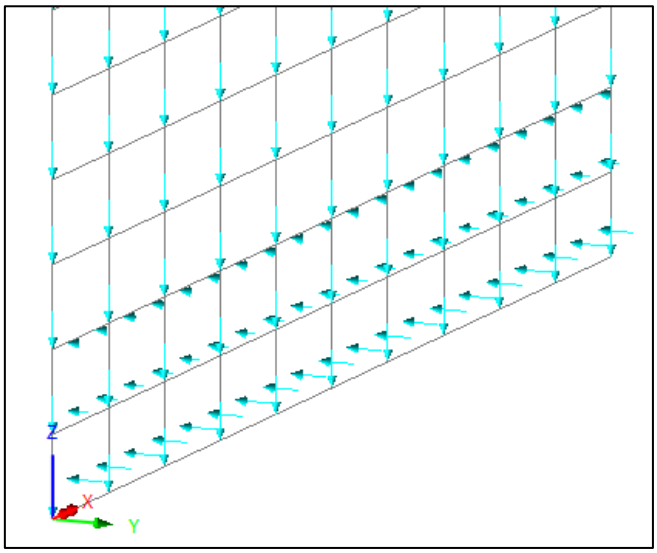

Figure 8: Discrete four node patch load applied to model representing hydrostatic loading from floodwater

The force per meter length of the wall is calculated using Equation 2 (Hamill, 2011). Although this is not required for the LUSAS model, it provides a value to compare hydrodynamic loading to in Section 2.8.1.

$$(\mathbf{2})\ Force = \rho * g * h_G * A = 1000 * 9.81 * 0.3 * (0.6 * 1) = 1.766\ kN/m$$

On solving the model, the maximum positive bending moment measured was 0.199kNm/m, observed at node 21, positioned on the horizontal area where maximum sagging was observed. The minimum bending moment was -0.057kNm/m, observed at node 220, in the centre of the bottom support, where hogging appeared to occur. The position of both node 21 and node 220 is detailed in Figure 9.

The maximum bending moment obtained from the model, 0.199kNm/m, is 90.9% that of the maximum value obtained using yield line analysis (0.219kNm/m, calculated in Section 2.1.1). It does however fit into the range of results obtained from the yield line analysis calculations, being closest to that obtained using lower diagonal yield lines at 45 degrees of height/width 1.2 meters (which produced a maximum bending moment of 0.202kNm/m). It would therefore seem reasonable that the model provides some validation to the yield line analysis. As with the yield line analysis results, the maximum bending moment obtained from the model is a viable result because it is lower than that obtained using approximate analysis assuming moments are only transferred vertically with pinned supports (0.947kNm/m) as calculated in Appendix E.

It is expected that the yield line solution or in this case the yield line pattern which produced the highest bending moment result (plastic analysis), would produce a higher maximum bending moment result than that obtained using a LUSAS finite element model (elastic analysis). This is because yield line analysis calculates the maximum bending moment in the plastic region, whereas the LUSAS FEA model will calculate the maximum bending moment in the elastic region. The panel will require a larger applied bending moment in order to undergo plastic deformation in comparison to elastic deformation, hence the use of yield line analysis would result in a higher maximum bending moment value.

Since the model seems to validate the hand calculations, the results of the model can also be used in the consideration of an appropriate yield line pattern, perhaps suggesting that for the scenario observed, the yield line pattern with lower diagonal yield lines of height/width of roughly 1.2m was most appropriate, since this pattern produced the closest bending moment value to that obtained from the LUSAS model. Alternatively, observing the bending moment contours (My) of the model, clearly indicates areas of the wall panel under the highest bending moment and therefore most likely to yield. The most prominent area of bending moment is a horizontal line roughly 0.7 meters from the base of the wall, as superimposed on the model bending moment contours in Figure 9. This corresponds closely to and therefore supports the yield line pattern depicted in Figure 6, which was believed to be the most likely failure pattern considering the conditions encountered (Kelman and Spence, 2003). Hence in future hand calculations in this study, a yield line pattern which appears to follow the most prominent bending moment pattern shown in the model bending moment contours (My) will be used. This is because it is thought this will be representative of a likely yield line pattern, which will be useful with more complicated and less researched alterations such as doors frames later in this study. This is possible since

in future analysis the FEA model will be produced first and yield line analysis will be completed afterwards for model validation.

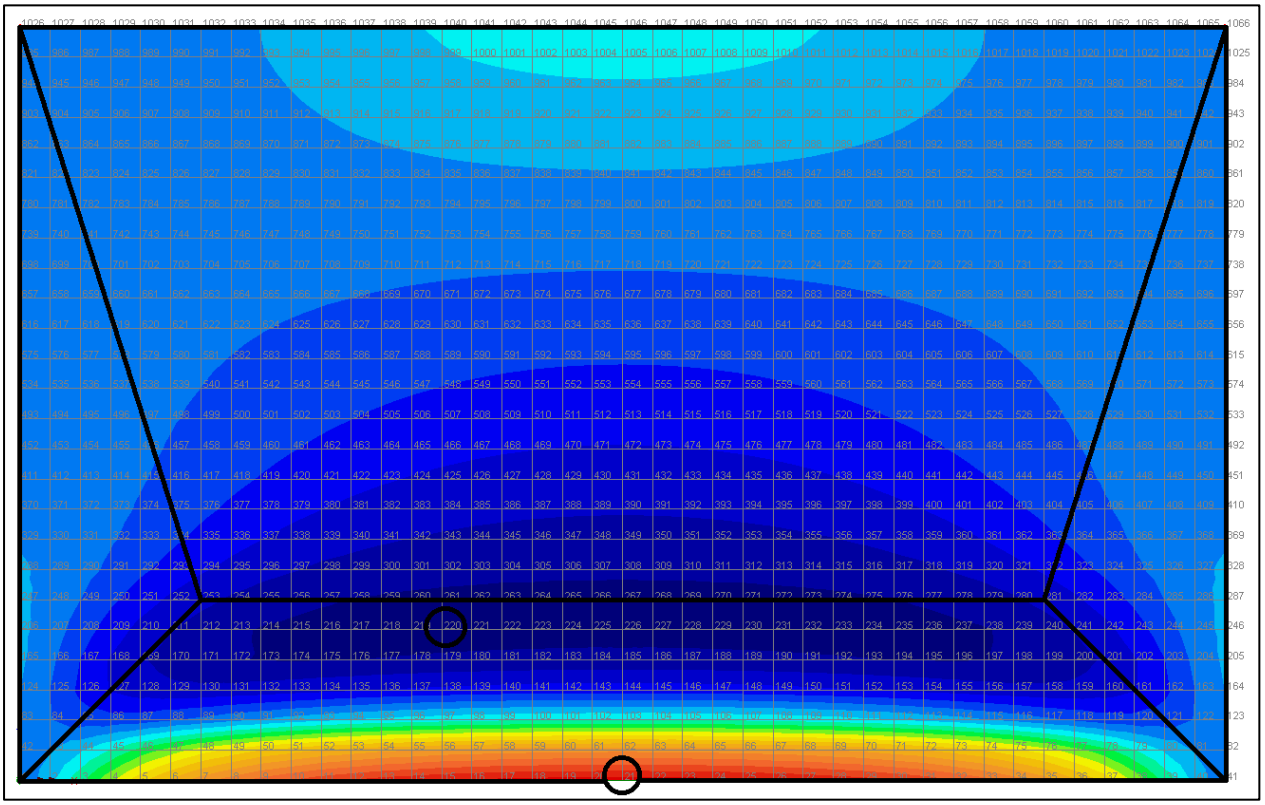

Figure 9: Model wall panel bending moment contours annotated with corresponding yield line pattern and indicating nodes with maximum and minimum bending moment

2.2. Altered widths

Whilst the unrestrained height of wall panels in domestic properties are generally similar; limited to the height of the ground floor, the width of panels can vary quite considerably. The width of a wall panel depends on features such as ties to columns, bonds to piers and bonds to return walls which provide suitable edge conditions (Morton, 1985). In the aim of identifying and understanding how factors can influence the maximum bending moment on a wall it is therefore important to analyse the relationship between increased panel width and maximum bending moment. In addition to the previously considered wall width of four meters, wall widths of one, two, six, eight and ten meters were considered. Kelman and Spence (2003) suggest that widths of one and six meters are relatively rare but represent extremes, so it was thought that the values chosen covered a broad range of realistic widths. All other parameters, including continuous supports and hydrostatic loading from 0.6 meters of floodwater were maintained as detailed in Section 2.1.

Using both FEA and yield line theory, analysis into the maximum bending moment in the panels with varying widths was undertaken.

2.2.1. LUSAS Model (FEA)

The LUSAS model used in Section 2.1.2 was altered for varying widths in addition to the previously examined width of four meters. Graph 2 below displays the resulting

maximum bending moment for each of these model variations and the results are also tabulated in Appendix F.

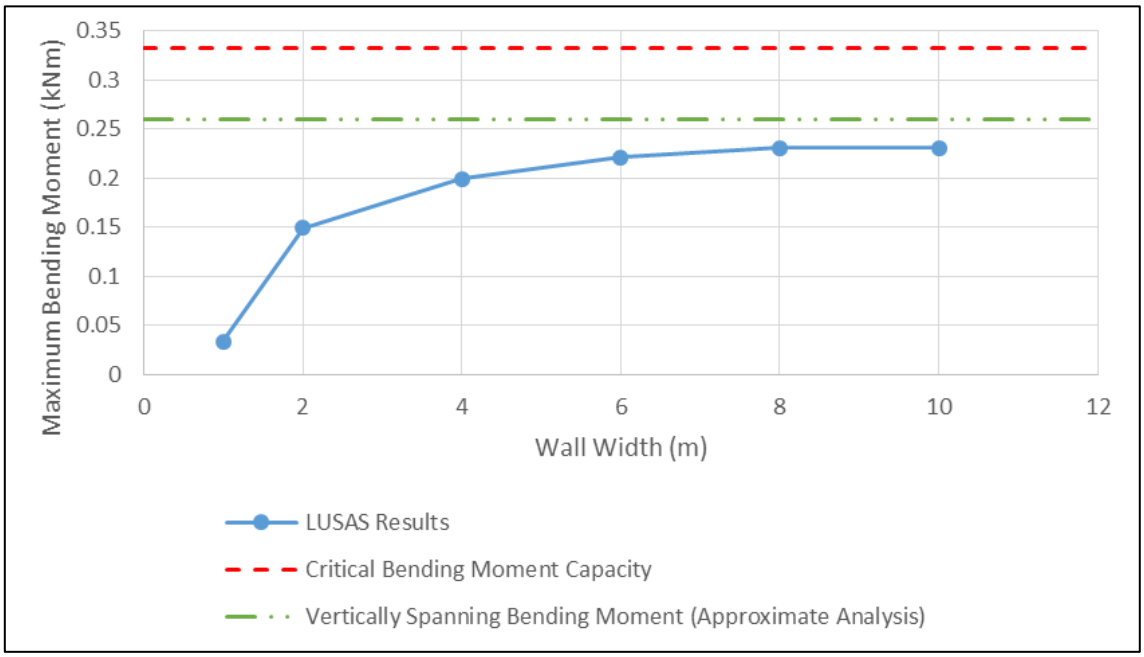

Graph 2: Maximum bending moment for varying panel widths obtained using LUSAS

It was expected that there would be logarithmic regression in the increase in maximum bending moment with increased panel width as seen in the correlation in Graph 2. This is because increased width results in increased bending moment being transferred vertically between the top and bottom supports rather than horizontally. By forcing the bending moment to span in one direction the maximum bending moment will increase, up to the point where full bending moment transfer occurs in the vertical direction.

The results for maximum bending moment for varied width (shown in Graph 2 and Appendix F) appear to tend to around 0.231kNm/m, which as discussed is expected to be the value of maximum bending moment when only transferred vertically. This was validated by modelling the panel as a beam fixed at both supports spanning vertically using approximate analysis, referring to the Steel Designers' Manual (as shown in Appendix G), resulting in a bending moment of 0.260kNm/m. The correlation between the experimental and approximate analysis results can be considered as good, with a difference of 0.029kNm/m. Some difference is expected and can be allowed for due to the assumption in the approximate analysis that the maximum bending moment occurs at 0.45 meters from the base (the multiple of 0.05m which provides the greatest bending moment), and some tolerance should allow for the *approximation* of approximate analysis.

Graph 2 indicates that the wall panel observed will not fail regardless of panel width, since the maximum bending moment the yield line results tend to and the bending moment calculated using approximate analysis considering full transfer in the vertical direction are 0.231kNm/m and 0.260kNm/m respectively. Both of which are lower than the moment of resistance of the panel which is calculated as 0.333kNm/m in Appendix B.

On inspection of the bending moment contour plots in LUSAS it can be seen that the area of maximum bending moment for the one meter width panel, with an aspect ratio of 0.25 (span divided by depth) spans vertically (see Figure 10), in contrast to all of the others where the area of maximum bending moment appears to span horizontally. Additionally, the position of the maximum negative bending moments in the one meter wide panel is on the sides rather than the bottom. This is due to the bending moment transfer being more pronounced horizontally between the side supports of the wall panel, when in the case of wider widths there is more pronounced transition of bending moment vertically between the top and bottom supports of the panel. This observation coincides with Chong's (1993) research which determined that for aspect ratios below 0.43, an area of bending moment can be observed spanning vertically, whereas for aspect ratios higher than 0.43, an area of bending moment can be seen spanning horizontally.

2.2.2. Yield Line Analysis Validation

In order to determine which yield line pattern best represented each wall width, the bending moment contours seen for each model were considered. Yield line patterns which follow the areas of maximum bending moment in the model were used, as described in Section 2.1.2. Hence there are differing lower diagonal yield line height/widths between the different wall panels, as detailed Appendix H where the results are displayed in a tabular format. The results of the yield line analysis validation are also displayed in Graph 3 below. Full yield line analysis calculations for each of the wall widths can be found in Appendix I.

Due to the observation that for the one meter wide panel the bending moment in the centre spans vertically rather than horizontally in the LUSAS model, the yield line pattern needed to be adjusted to account for this. A schematic of the yield line pattern used, as proposed by Chong (1993) can be seen below in Figure 10 superimposed on the bending moment contours for the model. As with the previous yield line patterns in this study, the lower diagonal yield lines were maintained at 45 degrees due to the reasons discussed in Section 2.1.1.

The yield line analysis validation revealed a fairly linear relationship between wall panel width and maximum bending moment. If further widths were examined it is expected that the maximum bending moment would also increase, continuing to display a graph with linear correlation. This is visibly different to the logarithmic regressive increase in maximum bending moment for the LUSAS results, as displayed in Graph 2. This demonstrates a limitation of yield line theory, since in reality the maximum bending moment will occur when there is full bending moment transfer spanning vertically (calculated as 0.260kNm/m in Appendix G). This limitation can be overcome however by appreciating that the maximum bending moment will occur when the bending moment only spans vertically, as calculated with approximate analysis. In order to do this only the yield line results below this vertically spanning approximate analysis value should be considered and results above this value should be assumed to equal to this value.

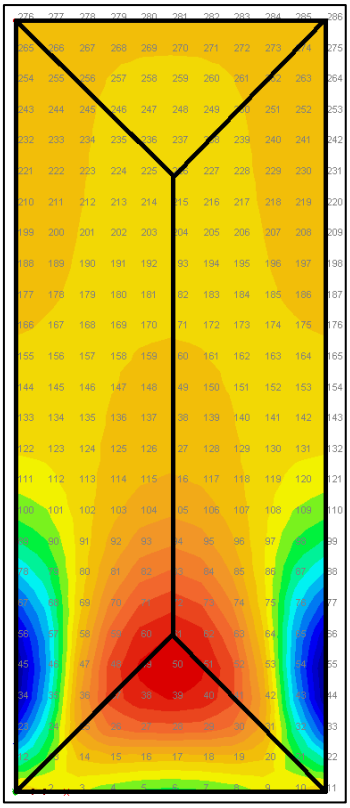

Figure 10: One meter wide model wall panel bending moment contours annotated with corresponding yield line pattern

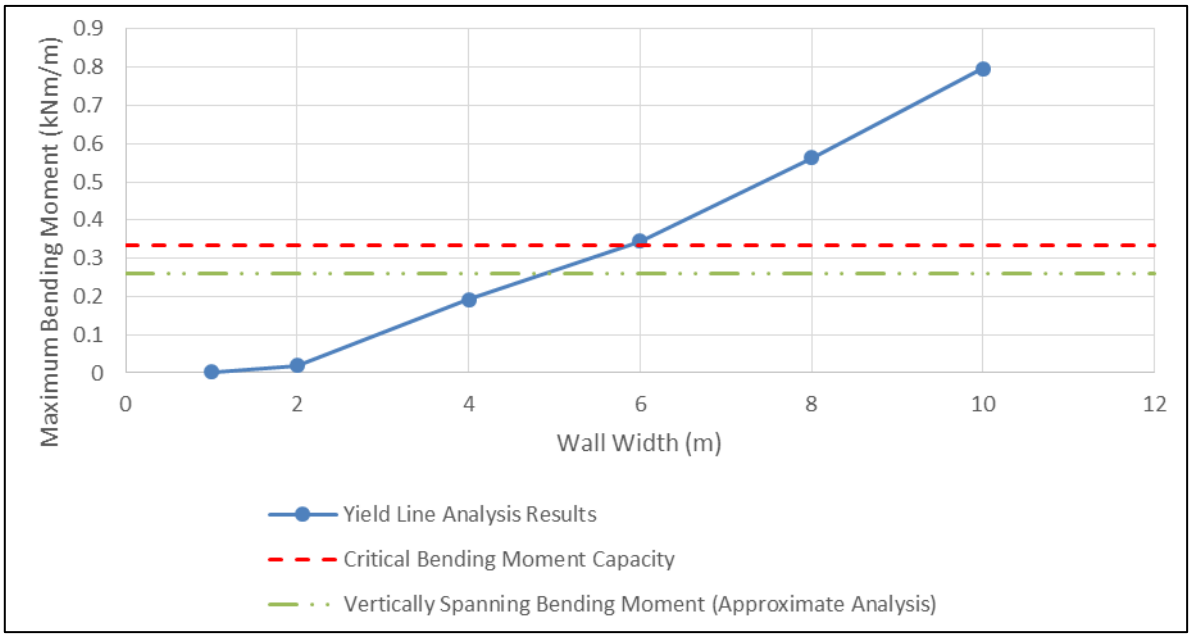

Graph 3: Maximum bending moment for varying panel widths obtained using yield line analysis

Referring to Graph 3 it can be seen that full bending moment transfer in the vertical direction occurs from a width of around 4.5 meters, calculated as 0.260kNm/m

(obtained using approximate analysis as calculated in Appendix G). This demonstrates that the wall panel will not fail regardless of width, since the moment of resistance of the panel is 0.333kNm/m (as calculated in Appendix B), as also seen with the LUSAS results.

On comparing the results from the yield line analysis to the LUSAS results it has been discussed that bending moments larger than in the case where the bending moment is only transferred vertically should be taken as this value instead. The bending moment values taken from the LUSAS and yield line results in Graph 2 and Graph 3 respectively are similar at larger widths, where the yield line results are taken as the vertically spanning bending moment, calculated with approximate analysis. Conversely however, the LUSAS and yield line results are different by a factor of ten for the one meter width panel. This indicates that whilst the LUSAS and yield line results may be quite different at smaller widths, the results of these different methods of analysis attune with increased width.

2.3. Altered support conditions

Continuous supports most accurately describe the support conditions seen in a residential property, therefore comparison of different support conditions may not provide relevant data (Kelman and Spence, 2003). However, it may be beneficial to analyse panels with free top edges to consider panels which are not load bearing, which presumably would be more likely to fail. Such panels may be present in domestic properties as external masonry leafs if the internal masonry leafs are load bearing, or to fill gaps between load bearing columns for example. The wall panel detailed in Section 2.1 was altered to have a free top edge.

Using both FEA and yield line theory, analysis into the maximum bending moment in the panels with fixed side and bottom supports and a free top edge was undertaken.

2.3.1. LUSAS Model (FEA)

The model described in Section 2.1.2 was altered to have a free top edge with all other edges fully fixed. This resulted in a maximum bending moment of 0.213kNm/m, 107% of the maximum bending moment resulting from all sides of the panel being fixed (0.199kNm/m).

Whilst smaller than expected, this increase in bending moment occurred because the top support becoming free would mean that a higher bending moment would have to transfer horizontally in order to take the load, to make up for less bending moment being able to span vertically.

2.3.2. Yield Line Analysis Validation

In the yield line calculations where all edges had continuous supports in Section 2.2.2, a yield line pattern similar to the one illustrated Figure 6 was used. However, Bhatt *et al.* (2014), Chong (1993) and Reynolds *et al.* (2008) suggests the use of yield lines patterns illustrated in Figures 11a and 11b for the case where one edge is free and the others are fixed. Kelman and Spence (2003) also propose the possible yield line pattern shown in Figure 11a, however they do not specify the corresponding support conditions.

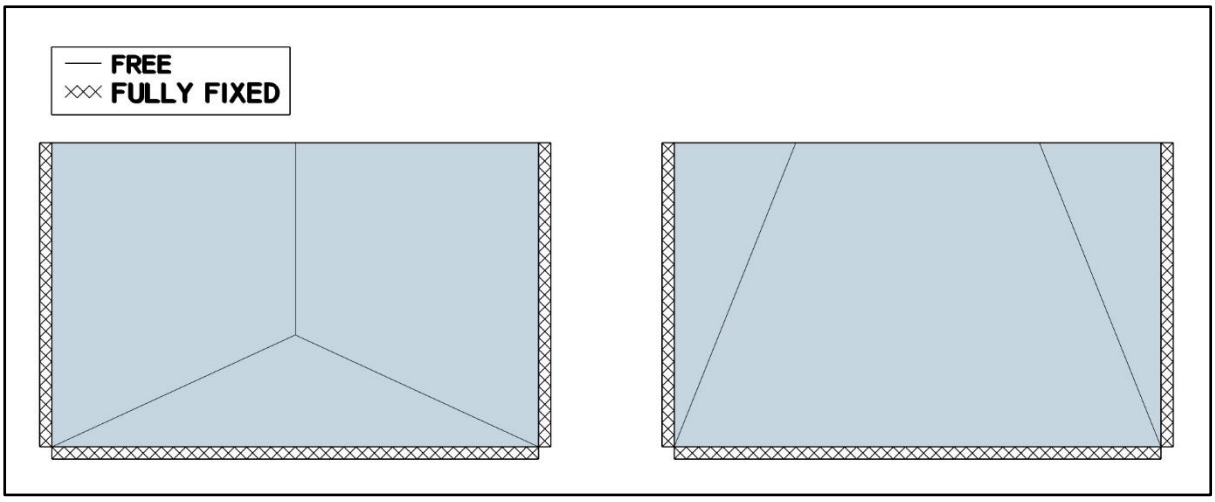

Figure 11a **Figure 11b**

- Yield line patterns for panels with free top edges

The yield line pattern which appears to follow the bending moment contours from the model described in Section 2.3.1 is superimposed on these contours in Figure 12. This yield line pattern appears to follow the same form as the yield line pattern seen in Figure 11a. Referring to the LUSAS model contours, there appears to be an area of maximum bending moment roughly 0.63m from the base of the wall panel, slightly lower than in the case where all edges had continuous supports. In order to acknowledge that the maximum bending moment appears 0.63m from the base of the wall, this is the location where all three central yield lines intersect. The maximum bending moment was calculated as 0.092kNm, and the calculations are shown in Appendix J.

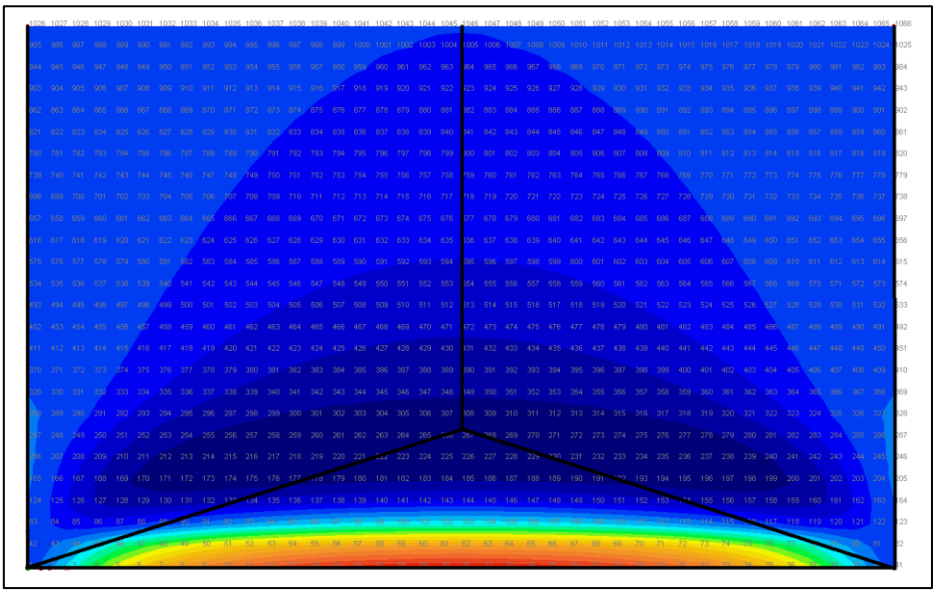

Figure 12: Bending moment contours for the model wall panel with a free top edge and the other edges fully fixed, annotated with a corresponding yield line pattern

This maximum bending moment value is considerably less than the values calculated for the same panel size with continuous supports. This result is clearly unrealistic since reducing the supports can only increase the maximum bending moment in the panel by restricting the transfer of bending moments in the vertical direction. This does not correlate with the LUSAS model results which showed increased bending moment when the top support condition was changed from fully fixed to free. This would indicate that this yield line pattern used is not the yield line solution, and further yield line patterns would need to be analysed in order to reach values close to or to obtain the yield line solution.

2.4. Addition of Openings and PLP Measures

All domestic housing includes doors and windows and many have sliding doors. In the aim of analysing the effect of flood water on domestic property walls it is therefore crucial to consider these. The use of PLP (property level protection) measures offers properties protection from flood water at the expense of increased loading on the frame and therefore masonry surrounding the opening in the form of strip loading. In order to gain an understanding of how these openings fitted with PLP measures impact the maximum bending moment applied to a wall, an average sized door, an average sized window and large patio sliding doors have been considered. In focusing on a few common opening types this should help maintain a focus to the testing, whilst indicating from the small selection of opening types chosen which of these result in the highest maximum bending moment from 0.6m head of water, as it is expected that the inclusion of frames will reduce the tolerable protection height (Morton, 1985). The panels with openings examined had the same size and characteristics as the panel detailed in Section 2.1.

Using both FEA and yield line theory, analysis into the loading on the panels with openings was undertaken.

Figure 13: A typical PLP measure (door barrier) used to prevent water ingress through a door frame (UK Flood Barriers Ltd, 2015)

2.4.1. LUSAS Model (FEA)

In order to replicate the use of PLP measures covering openings in masonry in the models, line loading was used where the openings were below the depth of the water, as shown in Figure 15. This allowed the simulation of the loading on the PLP barrier being transferred to the surrounding masonry. These line loads were applied to the panel, instead of a patch load with an inherent thickness, assuming the PLP barrier had no overlap onto the surrounding masonry, in consideration of the worst case. Furthermore, any support provided by a window frame or door frame to the surrounding masonry was ignored, hence the gap was modelled as empty, again in consideration of the worst case, since such frames are not usually load bearing features. Discrete patch loading was used to replicate the direct loading to the panel from flood water as detailed in Section 2.1.2. Figures 14a, 14b and 14c detail the dimensions of the model panels created in LUSAS, representing panels with a door, window and large patio sliding door frames respectively.

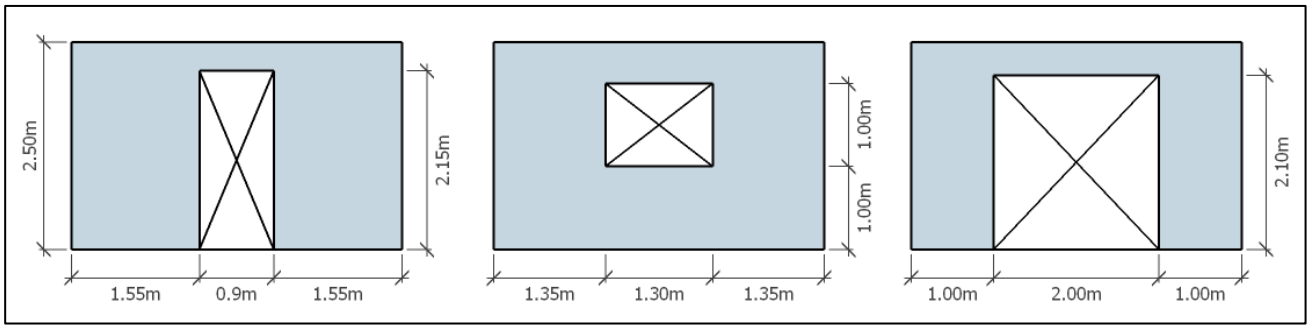

Figure 14a **Figure 14b** **Figure 14c**
- Schematics of the modelled openings for a door, window and large sliding door respectively

Symmetrical half models were created for each of the panels with openings, in order to have models as refined as possible. Where the two halves of the symmetrical models would meet along the centreline, the models were fixed in the x-direction to simulate the attachment of the other half of the model. Irregular triangular meshes were used to accommodate the irregular shape of the panels with openings.

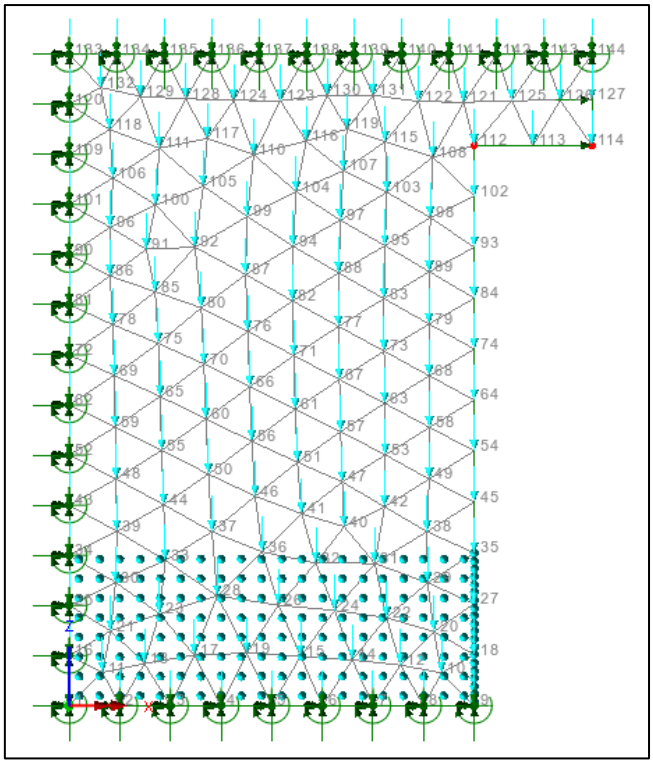

Figure 15: Symmetrical half model of the panel with a door opening, detailing the irregular triangular mesh, line loading, discrete patch loading and support conditions

The results of the LUSAS models are shown in Table 1 below.

Table 1: LUSAS results for wall panels with openings

Panel Feature	**Maximum Bending Moment (kNm/m)**
Door frame	0.220
Window frame	0.121
Large sliding doors frame	0.536

The maximum bending moment increased for both the door and large sliding doors frame in comparison to the plain panel modelled in Section 2.1.2 (0.199kNm/m) as expected. This is because the area in which bending moments can be transferred between the supports is reduced, as bending moment transfer can no longer occur across the opening. The maximum bending moment resulting from loading of 0.6m of water on the panel with the door frame was still less than the moment of resistance of the wall panel (0.333kNm/m, as calculated in Appendix B), suggesting that this panel would not fail. However, the maximum bending moment resulting from this same head of water on the panel with the large sliding doors frame was much higher than the moment capacity of the panel, suggesting that this panel would fail.

Unexpectedly the maximum bending moment for the wall panel with the window is less than for the same dimensioned panel without a window. This suggests that the opening for the window increased the ability of the panel to resist loading from flood water, which is obviously incorrect. This result advocates that a higher mesh

refinement may be necessary, beyond that allowable within the academic version of LUSAS.

2.4.2. Yield Line Analysis Validation

A different yield line pattern was required for each of the openings described in Figures 13a, 13b and 13c. The corresponding yield line patterns used are detailed in Figures 16a, 16b and 16c. Chong (1993) used the yield line pattern shown in Figure 16b in his work, and the other patterns have also been inspired from similar variations in his work.

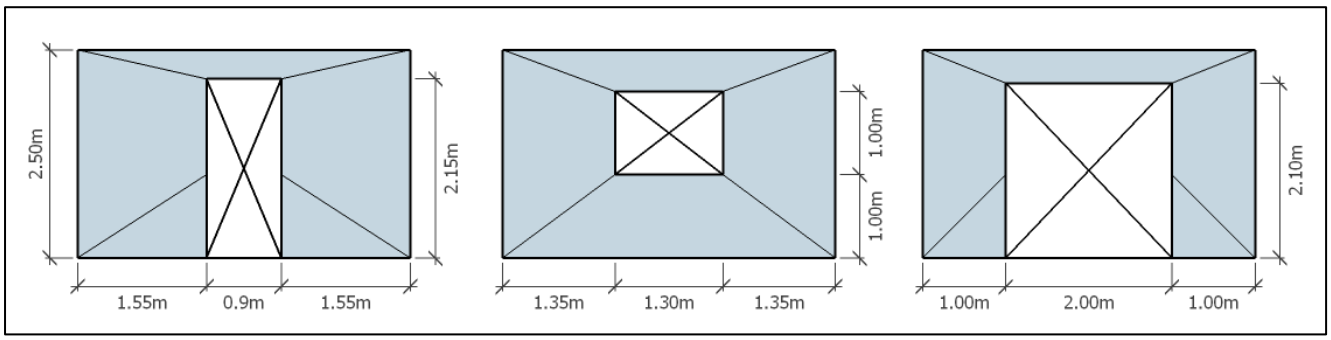

Figure 16a **Figure 16b** **Figure 16c**
- Yield line patterns used for openings in the panel for a door, window and large sliding door respectively

The results of the yield line analysis calculations are displayed in Table 2 below, and the full yield line calculations are located in Appendix K.

Table 2: Yield line analysis results for wall panels with openings

Panel Feature	**Maximum Bending Moment (kNm/m)**
Door frame	0.179
Window frame	0.139
Large sliding doors frame	0.174

In comparison to the same size panel without openings, which yield line analysis in Section 2.1.1 revealed had a maximum bending moment of 0.219kNm, all of the panels analysed with openings had lower maximum bending moments. This is obviously incorrect, since in reality the transfer of bending moments will be restricted, becoming more highly concentrated and increasing in maximum value. This may infer that the yield line patterns used and shown in Figure 16a, 16b and 16c are not appropriate for their corresponding openings.

2.5. Vertical Loading

Increased vertical loading will increase the flexural strength of a panel in the direction parallel to the bed joints, thus increasing the moment of resistance in this direction (Roberts and Brooker, 2013b). This is demonstrated in the following design moment

of resistance parallel to the bed joints equation (Equation 3), which was introduced in a pre-study project.

$$(\mathbf{3})\ M_{Rd,1} = \left(\frac{f_{xk1}}{\gamma_M} + \sigma_d\right) \times Z$$

Where,

- f_{xk1} = characteristic flexural strength of masonry bending about an axis parallel to the bed joints (dependant on mortar strength class and water absorption).
- γ_M= appropriate partial factor for materials.
- σ_d= design vertical load per unit area ($< 0.2 * \frac{f_K}{\gamma_M}$).
- Z = section modulus of the plan shape of the wall.

(Roberts and Brooker, 2013b).

The equation shows that further contribution to the design moment of resistance can be provided with increased design vertical load per unit area (σ_d). This loading can be applied from upper floors and/or the roof. However, in domestic housing there are usually only around two or three storeys, and light weight timber floors and roofs are common, limiting the applied vertical loading. Furthermore, not all of the walls in a property may be load bearing, potentially leading those which are not to yield under hydrostatic pressure first. Despite this, it is important to consider the effect of vertical loading on the design moment of resistance to gain a more rounded understanding of the effect of flood water on domestic properties, and to evaluate the potential benefits from vertically applied loading in terms of flood protection.

The panel considered in the analysis was the same as that described in Section 2.1. The inner leaf of the wall supported an area of 12m^2 from the floor above which was deemed realistic, and was tested for two typical residential unit floor loads suggested by Cobb (2014): 2.0kN/m^2 and 4.0kN/m^2, as well as a further loading of 1.0kN/m^2, 3.0kN/m^2 and 5.0kN/m^2 for a wider range of results. In analysing the effect of the five floor loads and comparing the same panel with no applied vertical loading it was hoped that a better understanding of the effect of vertical loading on the maximum bending moment could be established.

FEA was also used to analyses the stress in the panel resulting from the variety of vertical loads.

2.5.1. Moment of Resistance Parallel to Bed Joints Equation

The design moment parallel to the bed joints, $M_{rd,1}$, was calculated as follows using Roberts and Brooker's (2013b) equation (Equation 3), for a typical domestic unit floor load of 1.0kN/m^2 as follows.

In order to satisfy the equation, the design vertical load per unit area, σ_d, must be less than $0.2 * \frac{f_K}{\gamma_M}$, where f_K is the characteristic compressive strength of the masonry (Roberts and Brooker, 2013b). The calculation of f_K with the assumptions made can be found in Appendix L, where the value obtained was 1.87 N/mm^2.

$$\sigma_d = \frac{Loading\ (N)}{Wall\ area\ (mm^2)} = \frac{12 \times 1000}{4000 \times 100} = \frac{12000}{400000} = 0.03N/mm^2$$

$$0.2 * \frac{f_K}{\gamma_M} = 0.2 * \frac{1.870}{3} = 0.125N/mm^2$$

$$0.03 < 0.125 \ \therefore OK$$

$$M_{Rd,1} = \left(\frac{f_{xk1}}{\gamma_M} + \sigma_d\right) \times Z$$

$$M_{Rd,1} = \left(\frac{0.3}{3} + 0.03\right) \times \left(\frac{10^3 \times 100^2}{6} \times 2\right) \times 10^{-6} = 0.433kNm/m$$

(Roberts and Brooker, 2013a; Roberts and Brooker, 2013b)

Note: $\gamma_M$was taken as 3, since this is the worst case, assuming masonry with the lowest grade of units and the lowest class of execution control is used. $f_{xk1}$was taken as 0.3 due to the use of M4 mortar with clay units having a water absorption of over 12%.

The design moment parallel to the bed joints, $M_{rd,1}$, for a design vertical load of 2.0, 3.0, 4.0kN/m^2 was calculated in the same manner, with calculations shown in Appendix M. However, in the calculations it can be seen that the design vertical load per unit area resulting from the 5kN/m^2 loading exceeds the loading capacity of the masonry wall considered. Hence, the resistance moment afforded with this vertical loading has not been calculated. All of the design moment of resistance parallel to the bed joints results are illustrated in Graph 4 and tabulated in Appendix N, including the moment of resistance calculated for the same dimensioned panel without applied vertical loading.

Graph 4 clearly indicates that increased vertical loading dramatically increases the resistance moment of the masonry, with the design moment of resistance with 4kN/m^2 applied loading being over twice that with no applied vertical loading. There is a linear relationship between vertical loading and moment of resistance, with an average rate of increase of 0.1kNm/m moment of resistance for every increase of 1kN/m^2 of floor loading for the area considered.

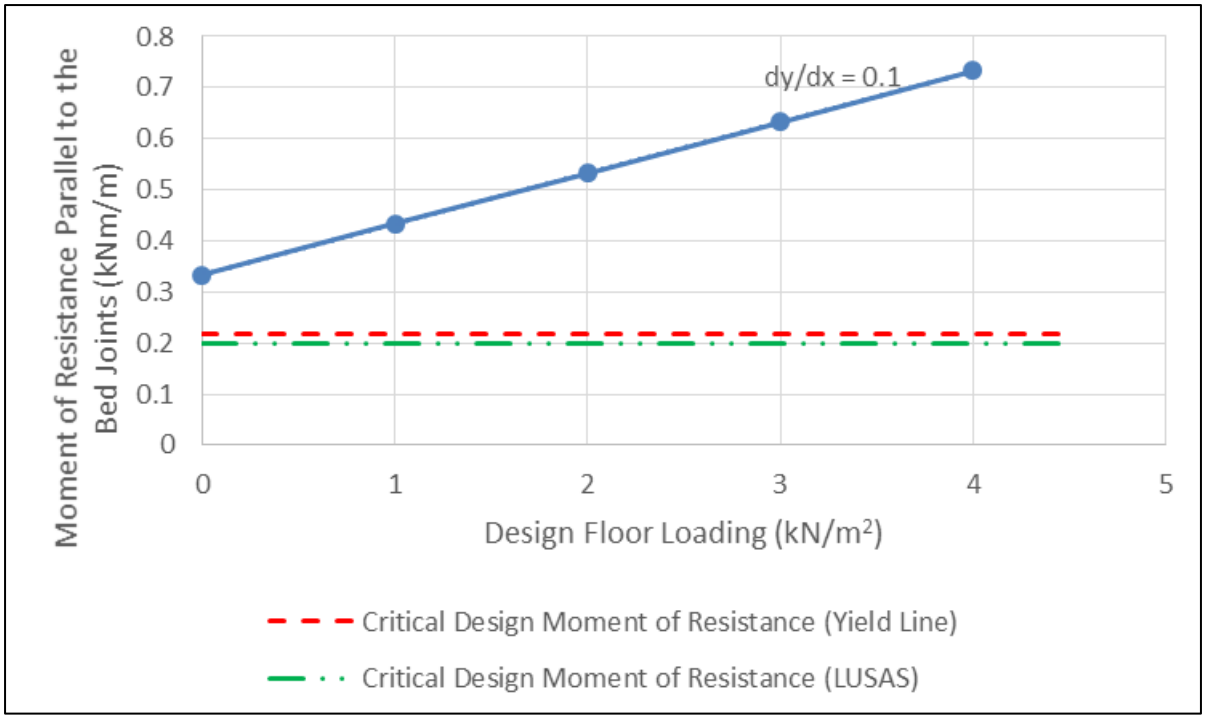

Graph 4: Moment of resistance parallel to the bed joints for varying design vertical loads

2.5.2. LUSAS Model (FEA)

3-D solid element models of the inner leaf (load bearing leaf) were created in LUSAS so that the stress inside the panel could be observed for each applied vertical load. The hydrostatic loading from the flood water was also applied to each model, although this is exaggerative of a two leaf wall as the outer leaf would assist in taking the loading.

Graph 5 below details the stress values for each of the applied loads, taken from resultant stress analysis (SE) conducted in LUSAS, all of which were recorded as compressive stresses. Graph 5 also details the ultimate limit state (characteristic compressive strength, f_K: 1.87 N/mm^2) and a very conservative serviceability limit state (0.35N/mm^2) compressive stress values for the masonry panel observed (Cobb, 2014).

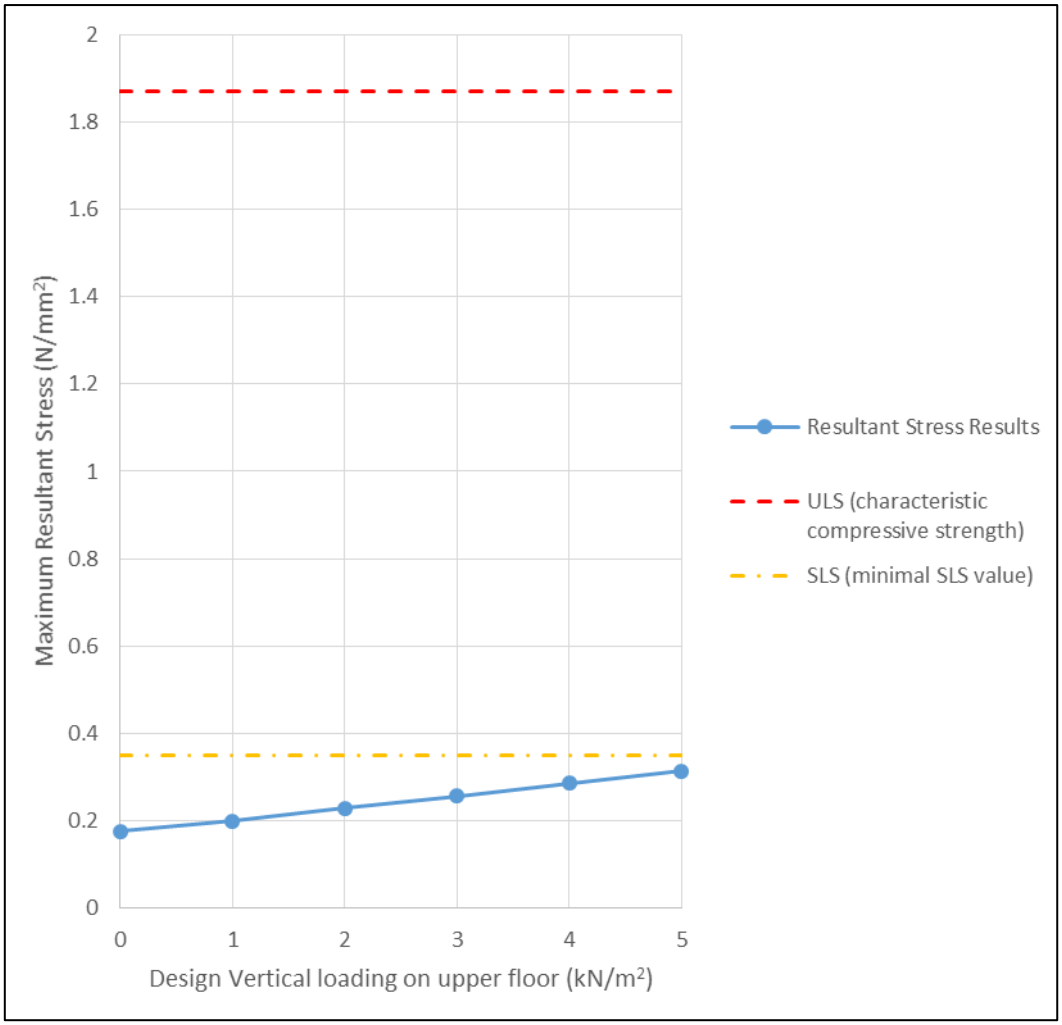

Graph 5: Maximum resultant stress results for varied vertical loading

Graph 5 indicates that increases in applied vertical load causes an increase in the maximum resultant stress (recorded as compressive stress), with a linear relationship. For each of the applied vertical loadings the resultant compressive stress was below the SLS (0.35N/mm^2) and therefore ULS limits, suggesting that the panel would not undergo structural damage (Cobb, 2015). However, the incline of Graph 5 appears to suggest that a further increase in applied vertical loading from an extra 1kN/m^2 on the supported floor area would cause the maximum resultant stress to exceed the SLS, perhaps resulting in some cracking.

The stress contours in Appendix O also indicate the presence of tensile stress in the masonry. However, the tensile stresses recorded for each of the vertical loads analysed where below the ULS characteristic flexural strength parallel to the bed joints of 0.4N/mm, suggesting that for the vertical loads analysed the wall panel would not fail (Roberts and Brooker, 2013b). With increased vertical loading and therefore compression throughout the panel the wall will have enhanced resistance to tensile stresses, demonstrated with reduced recorded tensile stresses (Cobb, 2015). Hence the panel seems unlikely to fail due to tension with any vertical loading, including the case where there is no vertical loading.

The position of maximum compressive stress and therefore maximum resultant stress for each of the applied vertical loadings is on the face of the panel opposite to the applied lateral hydrostatic loading near to the base, as annotated in Figure 17. This is due to the lateral hydrostatic loading, which causes the panel to rotate above its fixed support at the base compressing the masonry opposite the face of the applied loading and causing the face with the applied loading to undergo tensile stresses (Caprani, 2015). A schematic of this observed behaviour is shown in Figure 18 (where 'C' and 'T' corresponds to compressive stress and tensile stress respectively).

A print screen of the resultant stress contours (SE) for an applied vertical loading on the upper floor of 5kN/m^2 is shown in Figure 17 below, annotated to indicate the area of maximum resultant stress. Print screens of the resultant stress contours for the other analysed vertical loads are located in Appendix O.

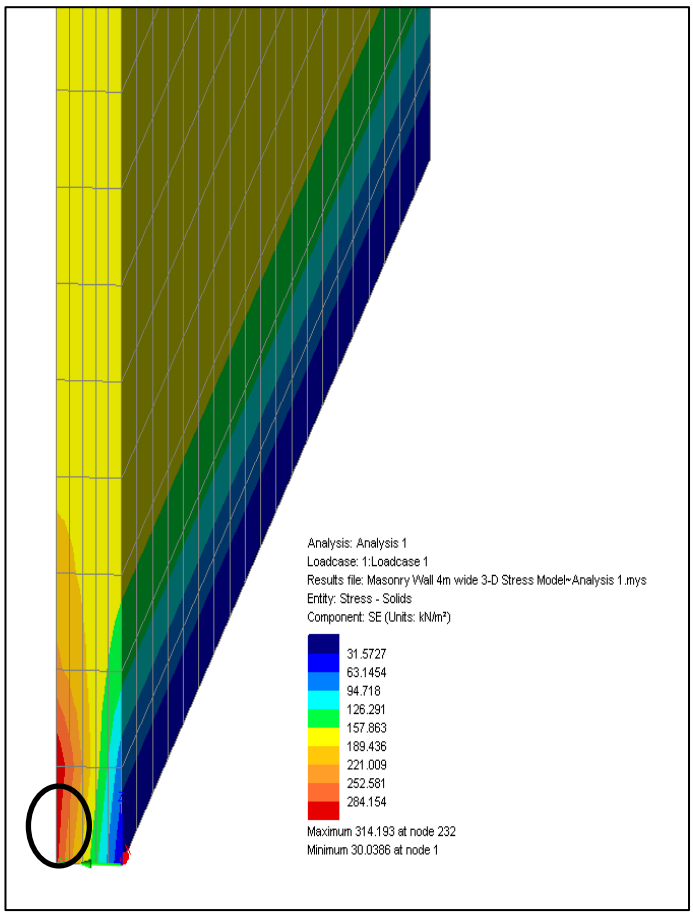

Figure 17: Resultant stress contours of the panel under applied vertical loading from 5kN/m^2 from the floor above annotated to indicate the area of maximum resultant stress

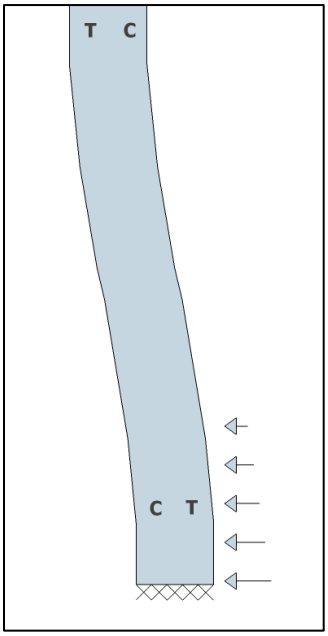

Figure 18: The location of compressive and tensile stresses in the panel as it deflects elastically

2.6. Masonry Construction

It has previously been considered in Section 2.5 that the moment capacity of a wall is in part determined by the thickness of the leaf or leafs, since the section modulus of a wall (*Z*) is required in the moment of resistance parallel to the bed joints equation (Equation 3). The thickness of wall leafs varies between properties, depending on whether brickwork or blockwork has been used and on the bonding pattern. In order to gain an understanding of how the masonry construction affects the moment capacity, five constructions have been considered; both single leaf and with two leafs, with varied thicknesses:

- Single masonry leaf: 100mm thick;
- Single blockwork leaf: 215mm thick;
- Inner and outer brickwork leaves: 100mm thick;
- Inner blockwork leaf: 215mm thick and outer brickwork leaf: 100mm thick;
- Inner and outer blockwork leaves: 215mm thick.

It was assumed that where applicable, both leafs of the wall could act together i.e. there would be effective wall ties, and other than the varied leaf thicknesses all other characteristics were the same as the panel described in Section 2.1.

2.6.1. Moment of Resistance Parallel to Bed Joints Equation

The design moment parallel to the bed joints, $M_{rd,1}$, was calculated as follows using Equation 3, for the five different construction types and therefore five different section moduli (Z). The results for the five wall constructions are shown in Table 3 below, in order of ascending design moment of resistance provided.

Table 3: Design moment of resistance afforded from varying section modulus

Inner Leaf Thickness (mm)	Outer Leaf Thickness (mm)	Section modulus (mm^3)	Design Moment of Resistance (kNm/m)
100	N/A	$1.667*10^6$	0.167
100	100	$3.333*10^6$	0.333
215	N/A	$7.704*10^6$	0.770
215	100	$9.371*10^6$	0.937
215	215	$1.541*10^7$	1.541

The results in Table 3 indicate that increases in leaf thickness increase the design moment of resistance substantially, with inner and outer leafs of 215mm thickness providing 4.6 times higher design moment of resistance than inner and outer leaves of 100mm thickness. On inspection of the results it can also be seen that design moment of resistance is directly proportional to the second moment area of the wall constructions, as is presented more clearly in Graph 6 below (annotated with the notation *inner leaf thickness*|*outer leaf thickness*).

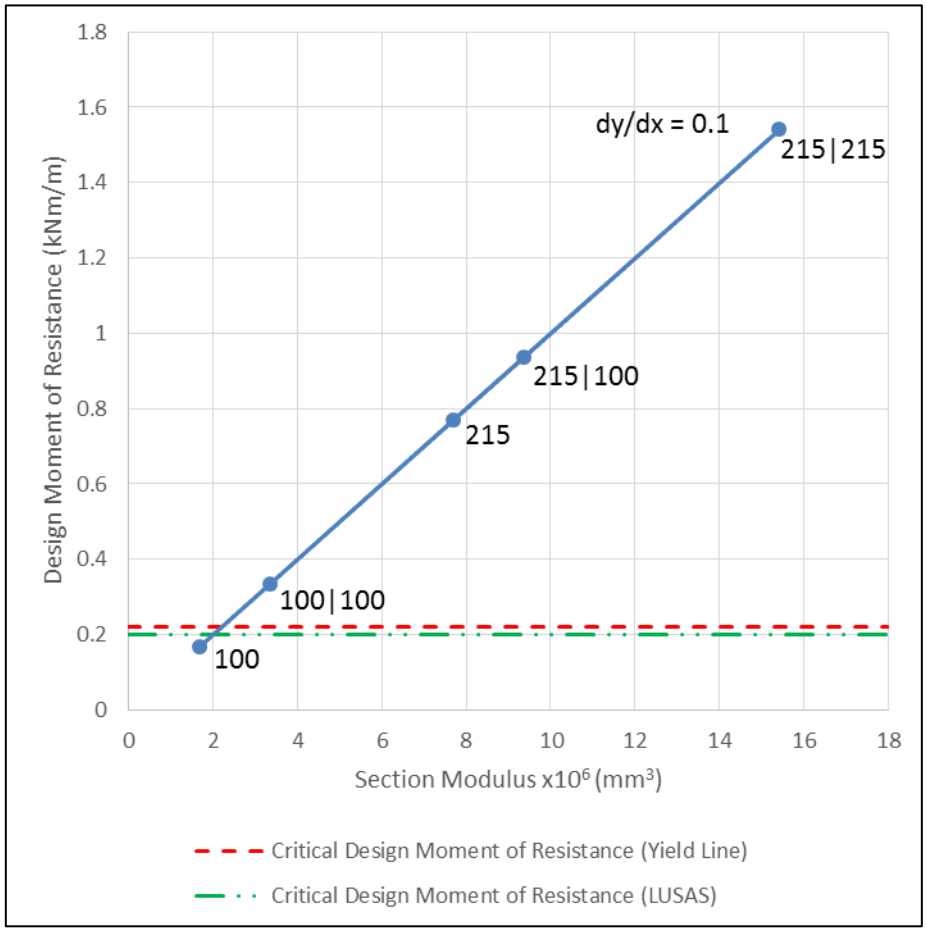

Graph 6: Moment of resistance parallel to the bed joints for varying wall constructions/section modulus

2.6.2. Comparison to LUSAS Model (FEA) and Yield Line Analysis

All of the wall constructions analysed, excluding the 100mm thick single leaf construction, had a design moment of resistance parallel to the bed joints which was higher than the applied bending moment from 0.6m of flood water. With the applied bending moment from the LUSAS model calculated as 0.199kNm/m in Section 2.1.2 and the maximum value from yield line analysis calculated as 0.219kNm/m in Section 2.1.1, both indicated in Graph 6. This suggests than only the single 100mm thick leaf wall would fail.

Since Graph 6 is linear, the section modulus with the corresponding critical moment of resistance can easily be read for both the LUSAS model and yield line results. For the maximum applied bending moment from the LUSAS model the critical section modulus is $2.0*10^6 mm^3$, and for the maximum applied bending moment from the yield line analysis the critical section modulus is $2.2*10^6 mm^3$.

2.7. Masonry Age and Condition

Whist the impact of vertical loading and masonry construction on the design moment of resistance has been analysed in Sections 2.5 and 2.6 respectively, ODPM (2003) suggests that age and condition are also factors to consider. The condition of masonry is subject to an accumulation of influences such as age, exposure and quality of workmanship. Whilst the condition of masonry is considered in Equation 3, through the appropriate partial factor for materials (γ_M), which considers class of execution and quality of units, there is no consideration for degradation of condition with age. This would mean that Equation 3 may not be appropriate for walls which are older and therefore of potentially poorer condition, unless a factor was used to consider the degradation of design moment of resistance caused due to depleting condition with age. This should consider exposure to the effects of water and weather penetration which can lead to degradation over time along with the durability of the masonry (Cobb, 2014). A degradation factor would be difficult to establish without results from physical testing. Furthermore, since the factors affecting the degradation of masonry with age will differ between buildings, due to varying levels of exposure, temperature changes and materials for example, in order to encompass the majority of domestic properties with one set of degradation factors, a strongly conservative approach will be required.

A review of relevant literature has revealed that research has not been undertaken into identifying factors to apply to the design moment of resistance equation to consider age and condition.

2.8. Hydrodynamic loading

So far in this study the loading on wall panels from hydrostatic loads has been considered, assuming the flood water imposing a load on the wall is static. It is common in flood events however for flood water to flow, which could result in hydrodynamic forces. At the same depth, hydrodynamic loading could be higher than hydrostatic loading, thus increasing the likelihood of wall panel failure. As part of this study it is therefore important to consider the effects of hydrodynamic loading on wall panels. The same panel detailed in Section 2.1 was analysed under hydrodynamic loading.

2.8.1. Hydrodynamic Loading Equation

Equation 4 can be used to calculate the hydrodynamic load per unit of exposed length:

$$(\mathbf{4})\ F = C_D * \rho * g * h * u^2$$

Where,

- C_D = coefficinent of drag.
- u = intensity of the velocity component orthoganol to the wall panel.

(Cuomo *et al*, 2008)

The drag coefficient is based on frontal area and effects the drag force (Hamill, 2011). Different shapes of the same frontal area have different drag coefficients, with higher values representing a shape which has greater drag. Drag coefficients are generally formed from the results of experiments in wind tunnels (Hamill, 2011). The closest comparison a wall panel has to shapes presented in drag coefficient tables is a flat plate at 90 degrees, which have drag coefficients ranging from between 2.0 and 2.3 (Auld and Srinivas, 2005; Hamill, 2011).

The intensity of the velocity component orthagonal to the wall panel will vary between flood conditions. In flooding typically seen in the Thames, a slow responding catchment, low velocities can be recorded at a given depth. Whereas in flash flooding typically seen in Boscastle, high velocities can be seen at the same depth. The hazard rating of flood water is a combination of velcoity and depth, and describes the danger the flood water presents. Hazard ratings displayed in matrix form, such as that seen in Appendix P, detail a number of differnet velocities and therefore hazard ratings at a given depth.

The drag coefficient can vary depending on the source of drag coefficient used and indeed the actual shape of the wall panel, whilst the intensity of velocity component orthagonal to the wall panel can vary in profile and between flood events. In order to gain a reasonable distribution of results for a wall panel given these variables, two drag coefficients were used in Equation 4, consisting of the upper and lower boundaries from the sources refered to. For each of these drag coefficients a number of hazard ratings for 0.6 meters head of water were taken from the matrix in Appendix P, which correspond to a range of velocities. The results of these calulations are displayed in Graph 7 below. The results are also tabulated in Appendix Q along with the factor of the value of the hydrostatic load per meter calculated in section 2.1.2 (1.766 kN/m).

Using Graph 7, it would be justifiable to assume that values in-between the two graphs for the upper and lower drag coefficients respresent reasonable hydrodynamic loads for the velocities displayed. In the case of hydrodynamic loading, providing a range of loads for given velocities is probably the best course of action due to the range of variables, including the drag coefficient and velocity profile as discussed, but also due to other variables such as the wider obstruction to flow, turbulance generated and flux profiles (Kelman, 2002). Depending on how well these variables are understood, a

conservative approach should be taken in the estimation of a reasonable hydrodynamic load.

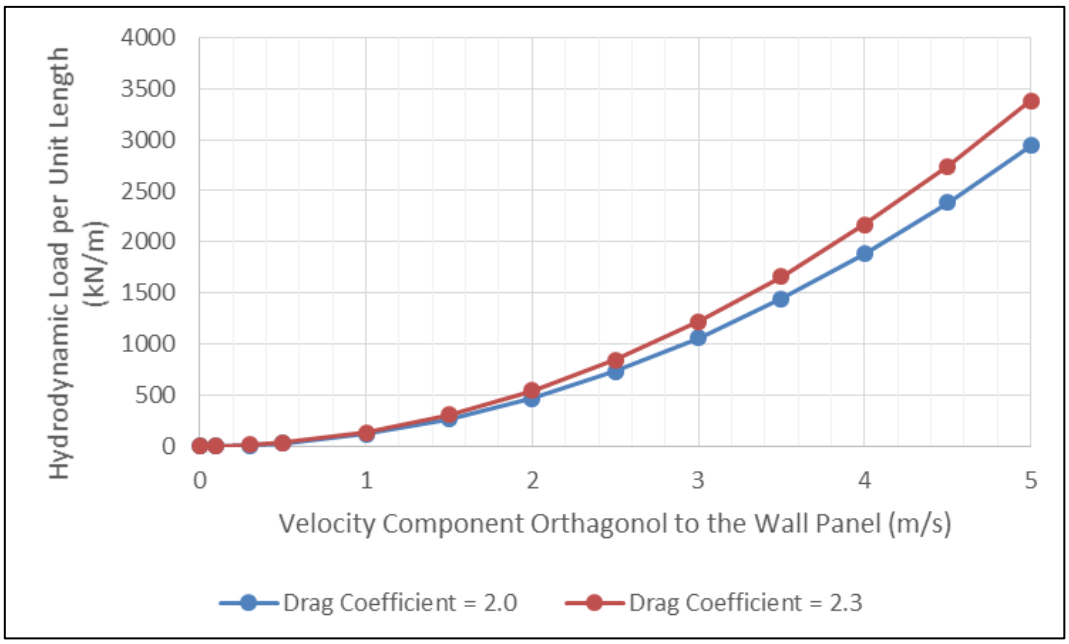

Graph 7: Hydrodynamic load per unit length for differing drag coefficient and velocity component orthogonal to the wall panel with 0.6 meter head

Whilst the changes in drag coeficient over the range of values selected did little to change the loading on the wall, increases in velocity had a relatively huge impact due to velocity being squared in Equation 4. Due to velocity being squared, increases in velocity caused the force on the wall panel per meter to increase exponentially, as shown in Graph 7. An alarming result from the calulations is that the force on the wall panel exerted by water with 0m/s and 0.1m/s orthagonal velocity for both drag coefficients using Equation 4 was less than that resulting from static water using Equation 2. This highlights that caution should be taken when using Cuomo *et al's* (2008) hydrodynamic load equation in the analysis of hydrodynamic loading on masonry wall panels, especially for slower velocities.

2.8.2. Yield Line Analysis

In order to compare the maximum bending moment resulting from varying velocities orthagonal to the wall panel and to see how these compared with the critical bending moment capacity of the panel, yield line analysis was carried out considering the increased loading. A factor of the increase in loading in comparison to the hydrostatic loading per meter calculated in Section 2.1.2 was used to increase the applied loading on the panel (the external work done in yield line analysis), as listed in Appendix Q. The results from the drag coefficient of 2.3 were used in order to provide more conservative results. The results are plotted in Graph 8, including the maximum bending moment gained from hydrostatic loading calculated in Section 2.1.1, and the calulations are shown in Appendix R.

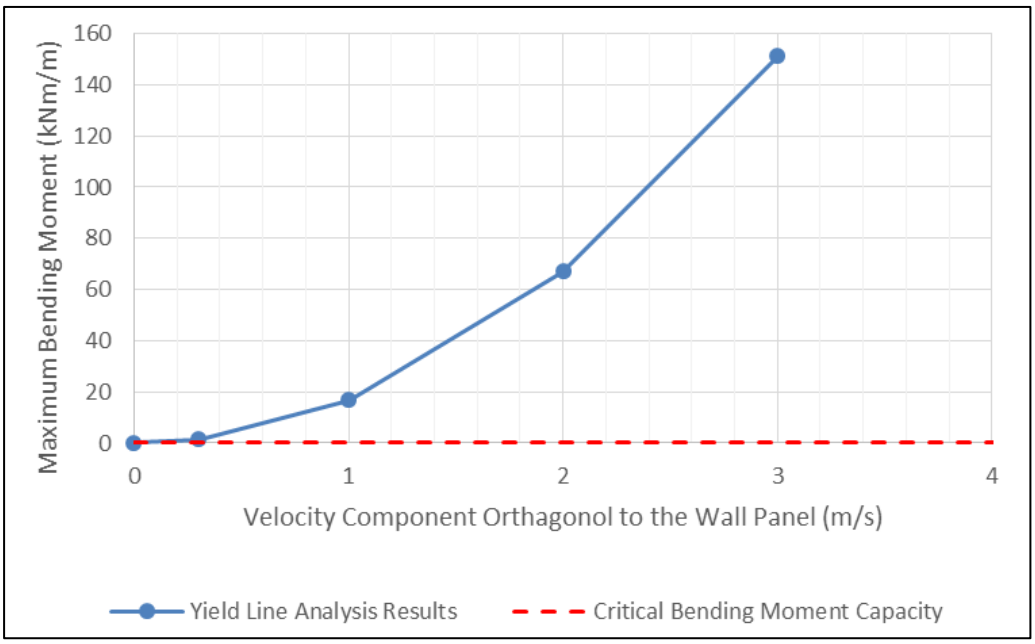

Graph 8: Maximum bending moment for varying velocity component orthogonal to the wall panel with 0.6 meter head obtained using yield line analysis

It is clear from Graph 8 that the maximum bending moment from relatively slow velocitites far surpasses the critical bending moment capacity of the wall panel (0.333 kNm/m), with flood water with an orthagonal velocity of 0.3m/s causing a bending moment around four times larger than the critical capcacity of the panel. It is also clear that as with the hydrodynamic load per unit length shown in Graph 7, the maximum bending moment appears to increase exponentially with increased velocity at the same depth as shown in Graph 8. Whilst Graph 8 provides an indication of the extent to which the critical bending moment capacity of the wall is surpassed, the graph in Appedix S is a focus on the lower velocities, which indicates that 0.03m/s is the critical velocity orthagonal to the wall panel.

3. Discussion

3.1 Original panel

The first analysis undertaken in this study, in Section 2.1, was a continuation of an analysis started in a previous project, analysing the plain wall panel detailed in Appendix A using both yield line analysis and a LUSAS model. Both of the maximum bending moment values obtained from the yield line analysis and the LUSAS model were below the design moment of resistance parallel to the bed joints of the wall panel, suggesting that the wall panel would not fail under loading from 0.6 meters head of water. This result was expected as the panel seemed fairly typical of domestic housing and did not have any features or properties which would presumably weaken the panel, such as openings or a notably wide width (both of which were later explored). Further testing was therefore required to see where the limits in the guidance lay.

3.2 Altered widths

The panel observed in the original analysis was altered with a number of different widths in Section 2.2. The relationship between width and maximum bending moment was plotted in Graph 2 and Graph 3 for the LUSAS and yield line analysis results respectively. Both the LUSAS and yield line analysis results demonstrated that the maximum bending moment in the wall panel increased with increased width, however trended towards a value where full moment transfer occurs in the vertical direction. This was clear from the LUSAS results as the results trended to this maximum value themselves, however the yield line results did not, and therefore reference had to be made to the vertically spanning bending moment calculated using approximate analysis, as the maximum bending moment value cannot exceed this value. Both the LUSAS and yield line results revealed that the panel observed would not fail regardless of panel width since the wall panel could resist the bending moment resulting from bending moment transfer purely in the vertical direction, which as discussed is the maximum possible bending moment for any width.

It is important to consider that wall panels with different heights and constructions may have a critical width when loaded with 0.6 meters of flood water. Action can be taken to reduce the width of wall panels in both new builds and existing domestic properties through the use of metal ties to columns, bonds to piers and bonds to return walls for example (Morton, 1985). Rather than reducing the width, another option is to reduce the effective height of wall panels through supporting the masonry with steel channels. Since flood water would apply the greatest loading towards the bottom of the panel these horizontal channels would be best placed towards the bottom of the panel, ideally where FEA highlights the highest bending moment.

3.3 Altered support conditions

In altering the top support condition from fixed to free, an increase in the maximum bending moment was observed in the LUSAS model as expected, since higher bending moment transfer was required in the horizontal direction in order to make up for less bending moment transfer in the vertical direction. The yield line analysis however resulted in a lower maximum bending moment with the top support being free rather than fixed. This result is clearly unrealistic since reducing the supports can only increase the maximum bending moment in the panel by restricting the transfer of bending moments in the vertical direction. It was decided that this was due to the yield line pattern used being inappropriate, and further patterns should be tested in order to identify the yield line solution. This links to the supposition made in Section 2.1.1 that yield line analysis should be used with caution and its suitability to specific scenarios must be assessed.

Whilst the LUSAS results reported an increase in bending moment in altering the top support condition from fixed to free, this increase was very small for the panel observed, being an increase of 0.014kNm/m, or 7%. The resulting maximum bending moment was less than the design moment of resistance of the panel suggesting that the panel would not fail. However, in the case of wider widths the maximum bending moment would presumably exceed the design moment of resistance for most domestic wall constructions. This is because previous analysis of altered widths in Section 2.2 revealed that bending moment transfer becomes more and more prominent in the vertical direction with increased width, trending to the point where bending moment

transfer is fully in the vertical direction. A free top edge would prevent bending moment transfer in the vertical direction, leading to further increase in the maximum bending moment.

Whilst the increase in bending moment for the panel with the free top support was small in LUSAS, this increase suggests that consideration needs to be made to the top support condition when determining safe protection heights for properties. However, this relatively small increase advocates that in order to increase the ability of a wall panel to resist flood water loading, other options should be considered before increasing the fixity of the top support, depending on panel width.

Whilst the support conditions for the sides may be considered as fully fixed due to the bonding to return walls for example and the bottom support may be considered as fully fixed due to the fixity to the foundations along with the effect of gravity, in reality the support condition of the top edge of a wall panel may be best described as in between fixed and free. This is because in the case where there is no vertical loading, the panel may be connected to the layer of bricks above or the roof with a horizontal layer of mortar and wall ties, rather than integrated into the brickwork of a return wall for example. In order to consider this using yield line analysis, an average of the maximum bending moment from the same panel with continuous supports and continuous supports with a free top edge could be taken. Alternatively, the level of fixity of the top support can be adjusted to the required amount using FEA software such as LUSAS. This was not conducted in this study because it was deemed more beneficial to test the worst case (free top support) in the interest of testing the current industry standard protection height.

3.4 Addition of openings and PLP measures

The inclusion of an opening for a door and large sliding doors with door barriers resulted in an increase in maximum bending moment as expected in the LUSAS results. The maximum bending moment with the opening for the door frame was below the critical moment capacity of the panel in the LUSAS results, suggesting the panel would not fail. However, in the case of the large patio doors, the maximum bending moment was beyond the panel capacity in the LUSAS results (being over 150% of the panel capacity), suggesting that the panel observed would fail.

In order to safely protect properties with large sliding doors such as that observed in this study, to the current industry protection height of 0.6 meters, the large resulting increase in bending moment needs to be managed. Some property level protection product manufacturers have appreciated this large increase in maximum bending moment in certain large door barriers by incorporating supports along the width of the openings which fit into pre-existing holes in the ground and take loading via cantilever action as seen in Figure 19. Alternatively, some barriers take loading along the bottom of the barrier, in addition to the sides, and transfer this load to the layer of bricks below the frame, as seen in Figure 20.

Figure 19: Barrier protecting large patio doors with a central support embedded into the ground (Stormguard, 2015)

Figure 20: Barrier mount connected to the brickwork below the patio door frame (Flood Wall, n.d.)

The case with the opening in the panel for a window produced lower maximum bending moment than the panel without any openings in the LUSAS results, which is obviously incorrect. If the panel was modelled as a horizontal slab there is the possibility that the maximum bending moment would reduce due to reduced self-weight, however as a vertical panel this will not be the case. Instead the inclusion of the opening will restrict the transfer of moments across the panel both horizontally and vertically increasing the maximum bending moment. It is thought that a higher mesh refinement is required in the model beyond the limits of the academic version of LUSAS in order to produce more reasonable results.

All of the panels with openings examined using yield line analysis revealed a lower maximum bending moment than the panel without any openings. Again this is obviously incorrect, and it is thought that the yield line patterns used were perhaps inappropriate. Further yield line patterns therefore need to be analysed in order to produce more reasonable results, perhaps using lower diagonal yield lines at alternative angles to the horizontal. Furthermore, yield line analysis was unable to consider the varying hydrostatic pressure across the panel due to the presence of door barriers, which in reality would transfer loading to the surrounding masonry as line loading. This again links to the supposition that yield line analysis should be used with caution and its suitability to specific scenarios must be assessed.

3.5 Vertical loading

Analysis of the effect of vertical loading on the design moment of resistance parallel to the bed joints revealed a substantial increase in resistance moment with applied vertical loading. Graph 4 indicated that this relationship is linear, with a 0.1kNm/m

increase in design moment of resistance parallel to the bed joints for every increase of 1kN/m^2 in floor loading (applied to the 12m^2 floor area supported). This linear relationship means that for the panel observed, estimating the resistance moment afforded from different applied vertical loads is very quick and easy. The design moment of resistance for any wall constructions and vertical loads could easily be calculated using the design moment of resistance equation in a spreadsheet.

The stress analysis undertaken in LUSAS using a solid element allowed the resultant stress throughout the entire inner leaf to be analysed. A key observation from this analysis is that the point of maximum stress for all of the applied vertical loads is compressive, and is located at the opposite side of the panel to the applied hydrostatic loading. This is because the panel rotates above the fixed bottom support due to the lateral hydrostatic loading, which with the combined effect of vertical loading causes material in this area of the panel to undergo compressive stress (Caprani, 2015). This maximum resultant compressive stress in the panel for each of the applied vertical loads was below both SLS and ULS limits, suggesting that the panel would not undergo structural damage. However due to the linear relationship of the resultant stress and applied vertical loading shown in Graph 5 it appears that a further increase of 1kN/m^2 (6kN/m^2) to the 12m^2 area of floor supported above would cause the maximum resultant compressive stress to exceed the SLS limit.

It is important to consider allowable vertical loading on masonry, since whilst the results suggest that increased vertical loading increases the design moment of resistance, this is limited by the vertical loading the masonry is designed for. This was demonstrated with the 5kN/m^2 loading, which was beyond the limitations of the masonry examined.

Whilst the maximum resultant stress in the panel was compressive and within SLS and ULS limits for the applied loadings considered, the stress contours in Appendix O also indicate the presence of tensile stress in the masonry. Whilst the tensile stress was lower than the maximum compressive stress, masonry does not perform as well in tension (Cobb, 2015). However, the tensile stresses recorded for the vertical loads analysed where below the ULS characteristic flexural strength parallel to the bed joints of 0.4N/mm, suggesting that for the vertical loads analysed the wall panel would not fail (Roberts and Brooker, 2013b). With increased vertical loading and therefore compression throughout the panel the wall will have enhanced resistance to tensile stresses, suggesting that the wall is less likely to fail due to tensile stresses with increased vertical loading (Cobb, 2015). Hence the panel seems unlikely to fail due to tension with any vertical loading, including the case where there a no vertical loading.

In new builds, allowing the masonry to bear loading could dramatically increase the design moment of resistance parallel to the bed joints, providing increased moment of resistance against hydrostatic loading from flood water. In consideration of existing properties, increasing vertical loading may not be viable or the most cost effective solution, where the masonry may not have the necessary design requirements, or major structural adjustments may be required.

3.6 Masonry construction

Several masonry and blockwork constructions were analysed using the design moment of resistance parallel to the bed joints equation. In comparison to the maximum bending moment applied from 0.6 meters head of water calculated from

both the yield line analysis and the LUSAS model in Section 2.1, it was revealed that of the constructions analysed only the 100mm single leaf panel would fail. Using Graph 6, the critical section modulus corresponding to the LUSAS model and yield line analysis maximum bending moments were calculated as $2.0*10^6 mm^3$ and $2.2*10^6 mm^3$ respectively. This corresponds to a critical depth of a single leaf panel of 110mm and 120mm for the maximum bending moment calculated using yield line analysis and the LUSAS model respectively. In order to be conservative the larger critical depth should be taken, resulting from the yield line analysis.

Whilst wall panels with increased section modulus will have increased resistance against applied loading from flood water, they will be costlier. This is because panels with increased section modulus will require more materials and presumably more labour in construction. Consideration into likely loading and cost would therefore be required to determine a suitable thickness of masonry leafs for particular properties. Whilst the costing has not been considered as part of this study, Graph 6 can be used to determine a suitable wall panel section modulus and therefore leaf thickness once the applied maximum bending moment has been calculated.

Increasing the section modulus of a wall panel could be a relatively cheap and effective way of increasing design moment of resistance in existing housing, in comparison to increasing the applied vertical loading as previously discussed. Whilst it may not be a visually attractive solution, the section modulus of a wall panel could be increased by increasing the thickness of the outer leaf with another layer of masonry. There are a number of practical issues which would need to be addressed however, including finding a suitable method of bonding the existing and new masonry and ensuring any airbricks are extended through the new layer of masonry. Alternatively, where space restrictions allow, a separate wall could be constructed away from the property in the aim of creating a dry moat during flooding, as can be seen in Figure 21. Although this potential solution carries the danger that failure of the external wall could result in sudden impact loading on the property walls, which could present a greater risk of damage.

Figure 21: Additional external wall for flood protection (California Department of Water Resources, n.d.)

3.7 Masonry age and condition

It was discovered that research has not been undertaken into identifying factors to apply to the design moment of resistance equation to consider age and condition of

masonry. Even if this research had been carried out it would be difficult to incorporate into consideration of domestic properties due to the extensive variety of construction and environmental exposure.

It could be argued that only masonry and blockwork within its design life is suited to lateral loading from flood water, due to the installation of PLP products for example, since the design moment of resistance of walls within their design life can be more accurately estimated. However, the status of domestic property wall design life will vary greatly, with the majority of homeowners unlikely to be familiar with the design life of their property walls. Instead the most appropriate approach to take seems to be to obtain assessment by a qualified building surveyor, architect or structural engineer for individual cases, in order to estimate the limits of loading from flood water (ODPM, 2003). This individual assessment could dramatically raise the costs of PLP schemes however, so highlighting particular properties with visible potential issues relating to age and condition for more detailed inspection could be more economic. This approach has been used in a number of recent PLP schemes, where a property survey is carried out prior to product installation. This practical approach is fitting, especially in consideration of the case of domestic properties which vary widely in age and condition.

3.8 Hydrodynamic loading

The final factor analysed as part of this study was hydrodynamic loading. Arguably this analysis produced results with the highest level of uncertainty due to the number of identified assumption and unknowns. However, an attempt was made to consider these through providing a range of results between boundaries, as shown in Graph 7.

In order to obtain results with higher reliability, more accurate estimates of the drag coefficient and velocity profile would need to be calculated, and other factors such as wider obstruction to flow, turbulence generated and flux profiles would need to be considered (Kelman, 2002). In reality this would most likely not be an economically viable solution for individual properties. Instead conservatively reducing the protection height for an area rather than individual properties, considering the effects of hydrodynamic loading would be more economical for government funded PLP schemes. For example, it should be considered that areas such as Boscastle which typically receive fast flows may be better suited to lower protection heights than areas such as the Thames which will typically receive slower flows for the same depth. However, assessing the effects of hydrodynamic loading for individual properties could still be an option for homeowners seeking private consultation.

Since the velocity of flood water had such a dramatic effect in increasing the applied bending moment on wall panels, methods of reducing the velocity of flood water around the proximity of a property could be an effective way of protecting walls from structural damage at increased protection heights. In both existing properties and in the design of new properties in urban areas, baffles, in the form of walls could be a relatively cheap method of slowing and diverting flows in the aim of reducing the velocity component orthogonal to property walls where total exclusion of flood water is not possible. This method could also provide the additional benefit of reduced peak hazard rating of the flood water, by spreading flow across a longer time, which would be especially useful in areas prone to flash flooding. Flood walls have been used to protect homes from flooding from the river Ouse in Selby (Dawes, 2011)

The graph in Appendix S allowed the ULS of the velocity component orthogonal to the wall panel to be estimated as 0.03m/s, with the current industry standard protection height of 0.6m. This value is very low highlighting the high influence velocity has on loading from flood water, although consideration should be made that this is a conservative result using a relatively high coefficient of drag value.

3.9 Is the current industry standard protection height appropriate?

Clearly from the discussed variables it is not possible to answer the question of whether the current industry standard protection height of 0.6 meters is appropriate with a definitive yes or no. Instead a more localised approach should be adopted, considering local conditions and variables as well as property characteristics. However, establishing protection heights which consider local conditions and variables as well as property characteristics will become more expensive the more detailed the investigations and surveys required are, and the more unique the protection offered between different properties is. A balance will therefore need to be struck between offering effective protection individual to the limitations of properties, and a method of implementing this which is practical and economic for use in PLP flood protection schemes across areas at risk of flooding.

Whilst the limits to the ability of a masonry panel to resist flood water has been explored in regards to the maximum applied bending moment and the design moment of resistance, a method of incorporating this into practice is required. The checklist in Appendix T aims to accomplish this by taking the limiting factors for a 0.6 meter protection height which were established in this Project (for the panel described in Section 2.1), and in simply asking yes or no, aims to determine whether this protection height is appropriate for a particular property. In the interest of being practical, some of the limits are simplified, for instance rather than specifying a specific orthogonal velocity limit in consideration of hydrodynamic loading (0.03m/s), only the question of whether notable velocities have been witnessed in previous events is asked. Since in the case of flood water velocity, it is unrealistic that a homeowner would have accurate velocity measurements, but would more likely have a visual memory of previous events. Because of this, this check sheet would be best suited to highlighting properties less able to resist flood water, and therefore where further inspection should be carried out by a qualified building surveyor, architect or structural engineer (ODPM, 2003). Since this extra investigation will come at a cost, in order to align the level of investigation to the funding available, a ranking system could be used, where the chosen top percentage of properties most likely to fail resisting 0.6 meters of flood water according to the check sheet are selected for further inspection, and the others are not. Other areas of study are required in order to enable the check sheet to incorporate a wider range of factors so that it is better suited at identifying properties at risk. Eventually a spreadsheet with factors identified in this Project and future studies would be able to identify properties unable to support 0.6 meter of flood water much more effectively.

An advance of a spreadsheet would be use of neural networks, where a number of rules, boundary conditions and worked examples of walls capable and incapable of resisting 0.6 meters of flood water would be entered. Based on this information the neural network would then be able to perform functional approximation in order to estimate whether submitted walls would be capable of resisting 0.6 meters of flood water (Lau, 1992). The use of a neural network would be well suited to this problem

solving which would involve high variety, due to their adaptive nature, allowing them to adapt to changes in data and learn the characteristics of input signals (Lau, 1992). The use of neural networks has its limitations however, since especially in the early stages of learning, validation may be required in order to correct errors in judgment made by the network (Lau, 1992). Although results would become more reliable as the network is trained, building up a larger and more varied database (Wasserman, 1989).

The limitations of wall panels in regards to the maximum bending moment obtained in this study could also be incorporated into design guidance by recommending ultimate limit states for the panel sizing analysed. As included in the check list in Appendix T, this Project has identified the ultimate limits of section modulus and orthogonal flood water velocity relative to a protection height of 0.6 meters. Other factors examined in this Project where upper limits have not been identified, but non-failure has, such as varying panel widths for the panel observed can also be used in the design of new wall panels and in the analysis of existing panels at risk of flooding.

Whilst advice is available and consultation services can be provided either funded through government schemes or privately, the protection height of properties is largely up to the individual property owners. It is therefore important that property owners are provided with information to enable them to make informed decisions and understand the risks, and expectations are appropriately managed. Whilst the limitations in regards to the maximum applied bending moment and design moment of resistance have been explored in this study, an effective method of presenting this information to homeowners needs to be established. Graph 2, 3, 5 and 8 all identify the ultimate limit state (ULS) for the observed wall panel, with Graph 5 also identifying the serviceability limit state (SLS). In producing a similar graph with information tailored to a particular property, this could allow a property owner to select a protection height below the ULS which they are comfortable with. By also including serviceability limit states (SLS), the homeowner will be able to get an even better idea of the likely extent of damage associated with the adoption of different protection heights.

3.10 Yield line analysis

The use of yield line analysis has been adopted in the continuation of the preliminary analysis in Section 2.1.1 as well as in the validation of subsequent LUSAS models, and has a number of advantages. Firstly, yield line analysis has an economical advantage over FEA software which can be very expensive, with a full licence of LUSAS costing thousands of pounds. This is because yield line analysis essentially only costs an engineer's time, and as long as yield line patterns are produced or checked by a suitably experienced engineer they can produce reasonable results. This may mean that in some scenarios, conservative use of the results obtained from yield line analysis is more economic than employing the use of FEA.

Secondly, although FEA software is arguably capable of providing more accurate results, these results cannot be used with confidence unless they are validated. The use of yield line analysis provides a quick and versatile method of validating FEA results, which can be carried out on site if necessary with only pen and paper.

Whilst some strengths of the use of yield line analysis have been identified in this Project, some limitations have also been identified. Firstly, in comparison to regular shaped slabs with uniformly distributed loads, the yield line solution for wall panels

under hydrostatic loading with features such as openings and varying support conditions can be less than obvious. This has been demonstrated in this Project, where in some cases the results from yield line analysis have been obviously incorrect, highlighting the need for further yield line patterns to be analysed outside of the scope of this Project. Hence yield line analysis may not be appropriate for more complicated scenarios unless an engineer has lots of experience in identifying yield line solutions for similar panels. Furthermore, in Section 2.1.1 it was considered that whilst the yield line solution should be that which provides the critical moment (the highest moment or least load capacity), there is a requirement to consider the appropriateness and likelihood of the solution given the "conditions encountered and the problem defined" (Goodchild and Kennedy, 2003; Kelman and Spence, 2003:60). These observations have led to a key supposition made as part of this Project that the reliable use of yield line analysis requires experience and "sound understanding of theory" in order to identify a likely failure mechanism (Caprani, 2006; Cobb, 2014:70). Where previously it was thought that a simple trial-and-error approach would be appropriate to find the critical moment, this is unsuitable given the findings of this study.

The second limitation of yield line analysis is that arguably this method of analysis does not accurately consider the material characteristics of masonry. This is because the theory is based on ductile behaviour and it is thought by some that masonry is too brittle for this theory to apply (Kelman and Spence, 2003). Furthermore, this analysis assumes that the material analysed is homogeneous and continuous, and does not take into consideration that in reality cracking in masonry would normally occur along the mortar joints due to the joints being weaker than the brick units (Brincker, 1984; Rafiq, n.d.). This cracking or yield line pattern would appear staircase-shaped as shown in Figure 22 below (Brincker, 1984; Kelman and Spence, 2003). This leads to the supposition that results from yield line analysis should be treated as approximations. This is fine in the aim of validating FEA models, but may suggest that a factor of safety should be used if yield line is to be the soul means of analysis. However, in support of the accuracy of yield line results, Goodchild and Kennedy (2003) mention that when walls are tested to failure, the collapse loads were compatible with the loads predicted by the yield line theory, a view supported by Morton (1986).

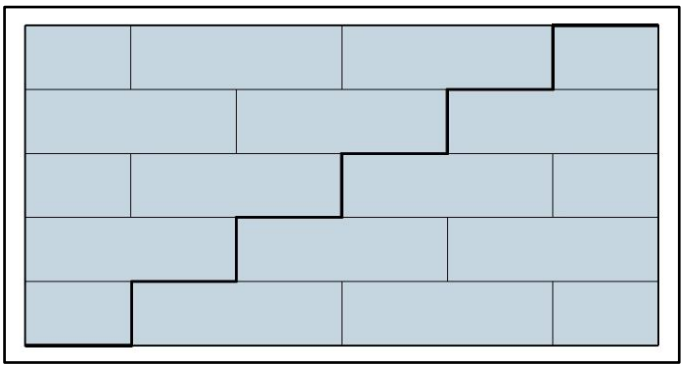

Figure 22: Yield line along the mortar joints

3.11 FEA model

FEA software was used to model wall panels and calculate the maximum bending moment or stress throughout this study. Whilst creation of the first model took longer than completion of a single yield line analysis calculation, subsequent results were produced much more quickly, since the initial model could easily be adjusted for alternative widths and support conditions etc. The use of FEA modelling had a further advantage in terms of speed, since for each FEA model created, the equivalent analysis using yield line analysis would often require numerous calculations in order to obtain a result in line with the yield line solution. If in practice maximum bending moment analysis was required on a number of similar panels, the increased speed of using FEA relative to yield line analysis could make FEA more economic.

Similarly to yield line analysis however, the FEA modelling conducted as part of this study has the disadvantage in that it assumes that the material analysed is homogeneous and continuous (since concrete was the most suitable material available in the academic version of LUSAS) (Brincker, 1984; Rafiq, n.d.). This will fail to take into account that in reality the cracking in masonry would normally occur along the mortar joints due to them being weaker than the brick units (Brincker, 1984; Kelman and Spence, 2003). It is however possible to model masonry joints in FEA, although this would take longer which would result in higher costs in practice. Instead it may be more economical to add a factor of safety to the FEA results (as suggested for the yield line analysis results) to allow for material limitations of the model.

4. Areas for further analysis

It is clear that further research is required to draw more conclusive results from some of the factors and variables considered in this study, mainly through applying the factors considered to a range of wall constructions. There are also a number of other factors and variables outside of the scope of this study which have been identified which require analysis in order to further understand the effect of flood water on domestic properties. This further study could help improve confidence into whether the current industry standard protection height is appropriate for different properties. The following items have been identified for further study:

- Investigation of further yield line patterns
- Modelling of flows for more detailed hydrodynamic loading
- Debris loading
- Wave loading
- Erosion
- Wider obstruction to flow
- Turbulence
- Flux profiles
- Physical modelling
- Modelling masonry as non-homogeneous

- Effect of damp proof coursing (DPC)
- Utilisation of spreadsheet
- Utilisation of neural network
- Buoyancy action

Throughout this study yield line analysis has been used where appropriate to calculate the applied bending moment applied to wall panels. As discussed in Section 2.1.1, the lower diagonal yield lines were angled at 45 degrees at the base of the wall because it was found that this is a common yield line angle, where permitted by the panel shape, which provides a fairly accurate distribution of loads (Goodchild and Kennedy, 2003). These lower diagonal yield lines were angled at 45 degrees at the base of the panel throughout all of the analysis in order to produce results which would be more easily comparable and to help maintain a focus to the research. However, there is a need to assess alternative yield line patterns, perhaps with yield lines at different angles, in order to gain results more aligned with the yield line solution. Such attempts were made in this study, as seen in Section 2.4.2, where the panels with the openings produced lower maximum bending moment than the same panel without an opening, which was obviously incorrect. In investigating further yield line patterns, appreciation should be made to the supposition made in this study that whilst the yield line solution should be that which provides the critical moment (the highest moment or least load capacity), there is a requirement to consider the appropriateness and likelihood of the solution given the "conditions encountered and the problem defined" (Goodchild and Kennedy, 2003; Kelman and Spence, 2003:60). Hence there is a reliance on "sound understanding of theory" in order to identify a likely failure mechanism (Caprani, 2006; Cobb, 2014:70).

Whilst a number of support conditions have been analysed in this study, there is still a number of other support conditions which exist in domestic properties which require analysis in order to gain a more rounded understanding of the effect of flood water. It has been discussed that the top support condition of wall panels which are not under the action of applied vertical loading may be best described as in-between free and fixed. In order to consider this using yield line analysis, an average of the maximum bending moment from the same panel with continuous supports and continuous supports with a free top edge could be taken. Alternatively, the level of fixity of the top support can be adjusted to the required amount using FEA software such as LUSAS.

The analysis of hydrodynamic loading in this study was believed to have the highest level of uncertainty due to the number of assumptions and unknowns identified, whilst an attempt was made to limit this through providing a range of results within boundaries. In order to produce results with a greater reliability, the various factors identified relating to hydrodynamic loading require further study. The factors linked to hydrodynamic loading identified in this study which require further research are: debris loading, wave loading, erosion, obstruction to flow, turbulence and flux profiles (Kelman, 2002). Physical modelling may be the most appropriate way of analysing these factors individually or in combination, due to their complexity, failing this computer modelling of flows may be required. Whilst the range of values for applied hydrodynamic force and bending moments could be narrowed, and SLS and ULS values could be established using factors of safety formed from this study and further

study, it would be near impossible to calculate exact values due to the inherent complexity and variety of hydrodynamic systems.

It has been discussed that the use of both yield line analysis and FEA in this study assumed that the masonry in the wall panels was homogeneous and continuous, and does not take into consideration that in reality cracking in masonry would normally occur along the mortar joints due to the joints being weaker than the brick units (Brincker, 1984; Kelman and Spence, 2003; Rafiq, n.d.). Furthermore, the effect of DPC's in masonry panels has not been considered, which could additionally increase the non-homogeneous nature of a domestic property masonry panel. Whilst Morton (1986) and Goodchild and Kennedy (2003) support the accuracy of yield line results when walls are tested to failure, having a more accurate representation of masonry in an FEA model should raise the accuracy of the results. Further to this, physical modelling such as that conducted by USACE (1988) on properties which were flooded in a controlled environment would provide the most realistic analysis.

It has also been discussed that the results in this study and future research into the effect of flood water of domestic property wall panels should be collated into a check sheet similar to the one seen in Appendix T, in order to help estimate for a given wall panel whether the current industry standard protection height of 0.6 meters is appropriate. A development of this could then be the creation of a spreadsheet, which could perhaps plot graphs with SLS and ULS boundaries, which in turn could be used as a tool for presenting information to homeowners so that they can make informed decisions as to how high to protect their properties. Further to the use of a spreadsheet, a neural network could be employed, which would be able to collect and use data to estimate for a given wall panel whether the current industry standard protection height of 0.6 meters is appropriate.

5. Conclusions

For the wall panel detailed in Section 2.1, analysis undertaken in this study arbitrates that the current industry standard protection height 0.6m is appropriate providing the velocity component orthogonal to the panel is less than 0.03m/s, there are no large openings and the panel is in a condition which would not compromise design flexural strength or material factor. This is because the panel section modulus, width, support conditions and vertical loading are all within the relevant ULS identified. However, areas have been identified for further study, including study of further yield line patterns outside of the scope of this study, in order to increase the confidence in this arbitration.

It was discovered that increase in wall panel width increases the maximum bending moment in a logarithmic regressive trend, trending to a limit where moment transfer occurs fully in the vertical direction, which was less than the ULS for the panel observed. For the wall panel observed, adjusting the top support condition from fixed to free, resulted in very little increase in the maximum bending moment, also maintaining a maximum bending moment below the ULS. Whilst it was found that research has not been undertaken into identifying factors to apply to the design moment of resistance equation to consider masonry age and condition, it was appreciated that consideration of masonry condition and age should be taken into account in adopting safe and effective protection heights.

Although many factors detrimental to the ability of a wall panel to resist loading from flood water have been identified, this study also determined that increase in design moment of resistance is afforded from vertical loading and increased leaf thickness for the wall panel detailed in Section 2.1.1. Taking advantage of the extra design moment of resistance these factors provides in both existing and new builds could dramatically increase the protection height within SLS and ULS boundaries. This could make the current standard industry protection height more applicable to more properties. Although it has been noted that there could be practical difficulties involved in increasing section modulus and the vertical loading on walls in existing properties.

In order to provide greatest protection to a property during a flood event using PLP measures, it has been discussed that a hybrid between a water exclusion and a water entry strategy should be adopted, minimising water entry whilst maintaining structural integrity (CIRIA, 2007). However, whilst providing thorough inspection of each property in order to tailor individual property protection heights would provide the best possible protection, it would not be economically viable as part of a property level protection scheme in industry. Instead it has been suggested in this study that an initial survey is carried out to highlight properties most likely to undergo structural damage if protected up to 0.6m, using a check sheet such as that in Appendix T. This check sheet would become more reliable with the inclusion of more ULS limits of the current industry standard protection height gained from further study. An advance of this would be the use of a spreadsheet and perhaps eventually neural networking, to gain increasingly quick and reliable arbitration as to whether the current industry standard protection height is appropriate for individual properties.

The use of FEA seemed to give reasonable results throughout the analysis undertaken within this study, with the exception of the analysis of the opening for a window. The inconsistency with the window model is thought to be because a higher mesh refinement was necessary, beyond that allowable within the academic version of LUSAS. This demonstrated that using a suitably refined mesh is key in producing reliable results using FEA. Whilst FEA proved to be a powerful tool for quick analysis of panels with many variations, the main disadvantage of this method of analysis if used in practice was found to be its high cost.

Testing a number of yield line patterns with the aim of obtaining a result in line with the yield line solution demonstrated the range of results yield line analysis can provide. The yield line analysis for a free top support condition and openings produced results which were lower than expected, leading to the observation that for less straight forward yield line patterns, many patterns may need to be analysed in order to obtain the yield line solution. These observations have led to a key supposition made as part of this study that the reliable use of yield line analysis requires experience and “sound understanding of theory” in order to identify a likely failure mechanism (Caprani, 2006; Cobb, 2014:70). Furthermore, there is a requirement to consider the appropriateness and likelihood of the solution given the “conditions encountered and the problem defined” (Goodchild and Kennedy, 2003; Kelman and Spence, 2003:60).

Whilst the wall panel detailed in Section 2.1.1 is deemed to be suitable for the current industry standard protection height of 0.6m according to the analysis undertaken as part of this study, the same cannot be said for all domestic property walls. This is due to the huge variety between domestic property walls, which includes panel width, vertical loading and construction for example, and limits have been identified within

this study which would suggest that some wall panels would not be able to withstand loading from 0.6m of flood water. It should be considered that the limits to the current industry protection height guidance determined in this study will of course differ between different wall panels in different properties due to the identified variables. Whilst the limits identified in this study can be used in industry as a guide for estimating the resilience of a wall panel to flood water, it is suggested that inspection is carried out by a qualified building surveyor, architect or structural engineer where wall panels are thought to test these limits (OPDM, 2003).

6. References

Auld, D. J. and Srinivas K. (2005) *Drag Coefficient*. Available at: http://www-mdp.eng.cam.ac.uk/web/library/enginfo/aerothermal_dvd_only/aero/fprops/introvisc/node11.html (Accessed: 4 January 2015).

Bhatt, P. *et al.* (2014) *Reinforced Concrete Design to Eurocodes: Design Theory and Examples* (4th edn.). London: Taylor and Francis.

British Standards Institution (BSI), 1997. *BS 8110-1: Structural use of concrete- Part 1: Code of practice for design and construction*. London: BSI.

California Department of Water Resources n.d. *Protect Your Property.* [image online] Available at: http://www.water.ca.gov/floodmgmt/lrafmo/fmb/fas/risknotification/links/pdfs/Protect_Your_Property.pdf?ContentID=13 (Accessed 2 November 2015).

Caprani, C. (2006). *Analysis and Design of Slabs*. Available at: http://www.colincaprani.com/files/notes/CED1/Design%20and%20Analysis%20of%20Slabs.pdf (Accessed: 8 October 2015).

Caprani, C. (2015). *Masonry Design*. Available at: http://www.colincaprani.com/files/notes/CED1/Masonry%20Notes.pdf (Accessed: 3 December 2015).

Chong, V. L. (1993) *The Behaviour of Laterally Loaded Masonry Panel with Openings.* Plymouth University: Unpublished.

CIRIA (2007) *Improving the flood performance of new buildings*. London: RIBA.

Cobb, F. (2014) *Structural Engineer's Pocket Book* (3rd edn.). London: Taylor and Francis.

Cuomo, G. *et al.* (2008) 'Hydrodynamic Loadings of Buildings in Floods', *Coastal Engineering,* 31, pp. 3744-3756.

Davison, B. and Owens, G. (2012) *Steel Designers' Manual* (7th edn.). Ascot: Steel Construction Institute.

Dawes, M. 2011. *Flood Wall River Ouse at Selby.* [image online] Available at: http://www.geograph.org.uk/photo/2627791 (Accessed 2 November 2015).

Flood Wall n.d. *Floodfix Patio Door.* [image online] Available at: http://www.floodwall.plus.com/Range/Standard_Barriers/a_floodfix_patio_door_white_50.jpg (Accessed: 2 November 2015).

Goodchild, C and Kennedy, G. (2003) *Practical Yield Line Design*. Surry: Reinforced Concrete Council.

Hamill, L. (2011) *Understanding Hydraulics* (3rd edn.). Basingstoke: Palgrave Macmillan

Kelman, I. (2000) *Coastal Settlement as Risk: Flood Vulnerability of Residential Properties in England.* [image online] Available at: http://www.ilankelman.org/phd.html (Accessed: 22 March 2015).

Kelman, I. (2002) *Physical Flood Vulnerability of Residential Properties in Coastal, Eastern England.* Cambridge University: Unpublished.

Kelman, I and Spence, R. (2003) 'A Limit Analysis of Unreinforced Masonry Failing Under Flood Water Pressures', *Masonry International*, Vol 16 (No 2), 1-11.

Lau, C. (1992) *Neural Networks.* Piscataway, NJ: IEEE (The Institute of Electrical and Electronics Engineers).

Morton, J. (1985) *The design of laterally loaded walls*. London: Brick Development Association.

ODPM (2003) *Preparing for Floods*. London: Office of the Deputy Prime Minister.

Rafiq, Y., n.d. Deep Beam & Shear Wall with Opening, *STAD505 Advanced Structural Engineering* [online via internal VLE], Plymouth University. Accessible through Plymouth University DLE. [4 October 2015].

Reynolds, Charles E.; Threlfall, Anthony J. and Steedman, James C. (2008) *Reynolds's Reinforced Concrete Designer's Handbook* (11th edn.). Oxfordshire: Taylor & Francis.

Roberts, J. J. and Brooker, O. (2013a) *How to design masonry structures using Eurocode 6*: *1. Introduction to Eurocode 6*. Surry: The Concrete Centre.

Roberts, J. J. and Brooker, O. (2013b) *How to design masonry structures using Eurocode 6*: *3. Lateral resistance*. Surry: The Concrete Centre.

Stormguard 2015. *Flood Barrier protecting large patio doors from flood water.* [image online] Available at: http://stormguardfloodplan.com/wp-content/uploads/2014/11/Flood-Barriers-protecting-large-patio-doors-from-flood-water5474677c1f458-1024x576.jpg (Accessed 2 November 2015).

Suresh, S. *et al.* (2008) *Supplementary note on flood hazard ratings and thresholds for development planning and control purpose.* Available at: http://evidence.environment-agency.gov.uk/FCERM/Libraries/FCERM_Project_Documents/FD2321_7400_PR_pdf.sflb.ashx (Accessed: 20 October 2015).

UK Flood Barriers Ltd. (2015) *UK Flood Barriers profile our extensive work in 2013.* [image online] Available at: http://www.ukfloodbarriers.co.uk/media.aspx?b=76 (Accessed: 25 August 2015).

USACE (1988) *Tests of Materials and Systems for Flood Proofing Structures*. Washington D.C., USA: USACE (US Army Corps of Engineers).

Wasserman, P. D (1989) *Neural Computing: Theory and Practice.* London: Van Nostrand Reinhold International Company Limited.

Appendices can be seen in Supplementary files in the list of Article Tools showing to the right hand side of the main window.